People's Democratic Republic of Algeria
Ministry of Higher Education and Scientific Research
Kasdi Merbah University – Ouargla
Faculty of New Information and Communication Technologies
Department of Electronics and Telecommunications

T H E S E

To obtain a master's degree in Automation and systems

Field: Science and Technology

sector: Automation

Specialization: Automation and Systems

Prepared by:

Bouzidi Islam

Topic

FUZZY LOGIC CONTROLLER BASED ON AN INDIRECT VECTOR CONTROL OF INDUCTION GENERATOR

Publicly defended before the jury composed of :

Name	Degree	Role
Mr. Benhelal Belkhir	MCB	President
Mrs. Ameur Fatima	MCA	Supervisor
Mrs. Souri Samira	MAA	Examiner

Academic Year 2024/2025

ACKNOWLEDGEMENTS

First and foremost, I thank and praise Almighty **Allah** for granting me the courage, determination, patience, and good health throughout these years, which enabled me to accomplish this work.

I would like to express my sincere gratitude and deep appreciation to **Professor Ameur Fatima** for her valuable guidance, and for the trust and support she extended to me throughout the course of this work.

I also extend my heartfelt thanks to all the members of the examination committee for kindly accepting to evaluate and review this work.

Finally, I wish to convey my deepest appreciation to everyone who supported and assisted me throughout my academic journey.

DEDICATION

I would like to express my sincere thanks and gratitude to:

My beloved parents, who have always been my true source of strength with their prayers, love, and unconditional support throughout every step of my journey.

My esteemed professors, especially my English professor, ***Romaissa Abdessamed***, who generously shared their knowledge with me and whose guidance has been a beacon throughout my academic career.

My dear friends, who stood by me through moments of struggle and joy, offering kind words and genuine encouragement.

To everyone who contributed with advice, encouragement, or even a simple smile

I dedicate this humble work as a token of appreciation for the support and kindness they have shown me along the way.

Islam

TABLE OF CONTENTS

Table of Contents

TABLE OF CONTENTS

TABLE OF CONTENTS

TABLE OF FIGURES

TABLE OF FIGURES

TABLE OF FIGURES

LIST OF TABLES

FUZZY LOGIC CONTROLLER BASED ON AN INDIRECT VECTOR CONTROL OF INDUCTION GENERATOR

Abstract:

This study focuses on the modeling and control of a Dual Star Asynchronous Machine (DSAM) integrated into a wind energy conversion system. In the first stage, a detailed overview of wind turbine technologies, components, and power characteristics is presented. The DSAM is then mathematically modeled in a two-axis reference frame using Park transformation, and its behavior is analyzed through voltage, magnetic, and mechanical equations.
Subsequently, an indirect vector control strategy is applied, allowing decoupled control of flux and electromagnetic torque via rotor flux orientation. To ensure optimal turbine operation and extract maximum wind power, a conventional PI speed controller is implemented. To improve system performance, a fuzzy PI controller is later introduced, enhancing adaptability under variable operating conditions.
Finally, simulations are carried out to compare the effectiveness of both control strategies. The results demonstrate the advantages of using fuzzy logic in speed regulation of DSAMs for wind energy applications.

Key words:

Dual Star Induction Machine, Flux Orientation, Fuzzy Logic, PI Controller, PWM Inverter, Simulation, Speed Optimization, Vector Control, Wind Turbine.

Résumé:

Cette étude porte sur la modélisation et la commande d'une machine asynchrone double étoile (DSAM) intégrée dans un système de conversion d'énergie éolienne. Dans un premier temps, un aperçu détaillé des technologies d'éoliennes, de leurs composants et de leurs caractéristiques de puissance est présenté. La DSAM est ensuite modélisée mathématiquement dans un repère à deux axes à l'aide de la transformation de Park, et son comportement est analysé à travers les équations électriques, magnétiques et mécaniques.

Par la suite, une stratégie de commande vectorielle indirecte est appliquée, permettant un contrôle découplé du flux et du couple électromagnétique via l'orientation du flux rotorique. Afin d'assurer un fonctionnement optimal de la turbine et d'extraire la puissance maximale du vent, un régulateur de

vitesse PI classique est mis en œuvre. Pour améliorer les performances du système, un régulateur PI flou est ensuite introduit, renforçant l'adaptabilité face aux variations des conditions de fonctionnement.

Enfin, des simulations sont réalisées pour comparer l'efficacité des deux stratégies de commande. Les résultats obtenus démontrent les avantages de l'utilisation de la logique floue dans la régulation de la vitesse des DSAM pour les applications en énergie éolienne.

Mots-clés :
Machine asynchrone double étoile, orientation du flux, logique floue, régulateur PI, onduleur MLI, simulation, optimisation de la vitesse, commande vectorielle, éolienne.

التحكم الاتجاهي والتحسين الغامض للسرعة في آلة حثية مزدوجة النجمة ضمن نظام طاقة الرياح

الملخص :

تهدف هذه المذكرة إلى نمذجة وتحكم آلة غير متزامنة مزدوجة النجمة مدمجة ضمن نظام تحويل طاقة الرياح. في المرحلة الأولى، يتم تقديم نظرة شاملة حول تقنيات توربينات الرياح، مكوناتها، وخصائص القدرة المستخرجة منها. بعد ذلك، يتم نمذجة الآلة رياضيًا في مرجع ثنائي المحور باستخدام تحويلة بارك، مع تحليل سلوكها من خلال المعادلات الكهربائية والمغناطيسية والميكانيكية .

في المرحلة التالية، يُطبق التحكم الاتجاهي غير المباشر، مما يسمح بالفصل بين التحكم في الفيض والعزم الكهرومغناطيسي عبر توجيه الفيض نحو محور الدوار. ولضمان التشغيل الأمثل للتوربين واستخلاص أكبر قدر ممكن من الطاقة، تم استخدام منظم تقليدي للتحكم في السرعة PI.

غامض (ضبابي) لتحسين أداء النظام والتكيف مع تغيرات ظروف التشغيل PI ثم تم إدخال منظم .

أخيرًا، تم إجراء محاكاة لمقارنة فعالية كل من طريقتي التحكم، وأظهرت النتائج تفوق التحكم بالمنطق الضبابي في تنظيم سرعة الآلة الحثية ضمن تطبيقات طاقة الرياح .

الكلمات المفتاحية :

آلة غير متزامنة مزدوجة النجمة، توربين ريحي، محول PWM،التحكم الاتجاهي، توجيه الفيض، المنطق الضبابي،

منظم PI ، تحسين السرعة، المحاكاة .

LIST OF SYMBOLS

Symbol	Description	Unit
L_{s1}	Self-inductance of the 1st star	H
L_{s2}	Self-inductance of the 2nd star	H
L_{mr}	Maximum value of rotor mutual inductance coefficients	H
L_r	Self-inductance of one rotor phase	H
L_{ms}	Maximum value of stator mutual inductance coefficients	H
L_{sr}	Maximum value of mutual inductance between one stator and rotor phase	H
ω_{coor}	Rotation speed of the (d,q) reference frame with respect to stator 1	tr/min
ω_r	Rotation speed of the reference frame (d,q) with respect to rotor	tr/min
Ω_m	Mechanical rotation speed of the rotor	rad/s
θ1	Rotor position with respect to stator 1	(°)
θ2	Rotor position with respect to stator 2	(°)
a	Angle between stator 1 and stator 2	(°)
M	Modulation index of the inverter	Unitless
R	Inverter control ratio	Unitless
ω_s	Stator electrical angular speed	rad/s
ω_r	Rotor electrical angular speed	rad/s
P	Number of pole pairs of the machine	Unitless
φ_r	Rotor flux	Wb
R_r	Resistance of one rotor phase	Ω
R_{s1}	Resistance of one phase of the 1st star	Ω
R_{s2}	Resistance of one phase of the 2nd star	Ω
T_r	Rotor time constant	s
a_{s2}, b_{s2}, c_{s2}	Indices corresponding to the three phases of stator 2	Unitless

LIST OF SYMBOLS AND GLOSSARY

a_r, b_r, c_r	Indices corresponding to the three phases of rotor	Unitless
P	Laplace operator	Unitless
P_t	Wind power	W
P_w	Aerodynamic power	W
P_{mec}	Mechanical power	W
P_n	Nominal power of the generator	W
I_{dc}	DC bus current	A

GLOSSARY

Abbreviation	Meaning
DSAM	Double Star Asynchronous Machine
MCC	Direct Current Machine
FOC	Field Oriented Control
OP	Optimal Point
PWM	Pulse Width Modulation
MPPT	Maximum Power Point Tracking
VN,N,SN,Z,SP,P,VP	Very Negative, Negative, Slightly Negative, Zero, Slightly Positive, Positive, Very Positive respectively

GENERAL INTRODUCTION

GENERAL INTRODUCTION

The renewable energy industry has experienced unprecedented growth in recent decades, with wind energy emerging as one of the most significant sources of clean and sustainable power. As global energy demand continues to rise alongside increasing environmental awareness, the development of highly efficient and reliable wind energy conversion systems has become a paramount priority for researchers and engineers worldwide.

Wind turbines constitute the fundamental core of wind power generation systems and have undergone substantial technological advancement in control and operation methodologies. Among the modern technologies employed in this domain, the utilization of Dual Star Asynchronous Machines (DSAM) represents an innovative solution that offers numerous advantages over conventional machines, including enhanced performance, increased reliability, and reduced harmonic distortion.

Effective control of these systems requires advanced strategies that ensure maximum utilization of available wind energy while maintaining system stability and operational integrity. Vector control emerges as a fundamental technique for achieving superior performance in asynchronous machines, while fuzzy logic provides intelligent solutions for handling uncertainty and variations in operating conditions.

The primary objective of this study is to develop and analyze advanced control systems for dual star asynchronous machines in wind energy applications. Through the integration of vector control techniques with fuzzy logic methodologies, this research aims to optimize energy extraction efficiency and enhance overall system performance.

This study comprises three main chapters:

- **Chapter One** : focuses on the mathematical modeling and analysis of the dual star asynchronous machine, presenting various wind turbine technologies and power characteristics, while developing comprehensive mathematical models for the machine and PWM control systems.

- **Chapter Two** : addresses the implementation of vector control techniques and speed optimization for the machine in wind energy systems, emphasizing strategies for maximizing wind power extraction and improving the dynamic performance of the system.

- **Chapter Three** : explores the application of fuzzy logic in control systems, developing intelligent controllers based on fuzzy logic techniques to enhance system response and effectively handle variations in operating conditions.

Through this research, we endeavor to contribute to the development of advanced technical solutions that enhance the efficiency and reliability of wind power generation systems, thereby supporting global efforts toward the transition to renewable and sustainable energy sources. The integration of sophisticated control strategies with innovative machine configurations represents a significant step forward in optimizing wind energy conversion systems for future sustainable energy applicate.

CHAPTER 1

INTRODUCTION OF WIND TURBINE AND MODELING OF DSAM

1.INTRODUCTION

Wind energy is one of the leading renewable energy sources that has experienced rapid global growth in recent decades, thanks to its clean, sustainable nature and minimal environmental impact compared to fossil fuels. It operates by converting the kinetic energy of wind into electrical energy through the use of wind turbines. Historically, wind power was used for tasks such as water pumping and grain milling, but in modern times, it has evolved into a major source of large-scale electricity generation. Wind energy systems range from small, standalone (off-grid) units used in remote areas to large, grid-connected installations that help supply power to cities and industrial zones.

Between 1846 and 1908, Paul La Cour conducted experiments using wind turbines to drive a DC generator for electricity production. Later, during the winter of 1887–1888, American inventor Charles Francis Brush built the first wind turbine coupled with a 12 kW electrical generator to power his home, using a battery system for energy storage (Figure I.1) [1].

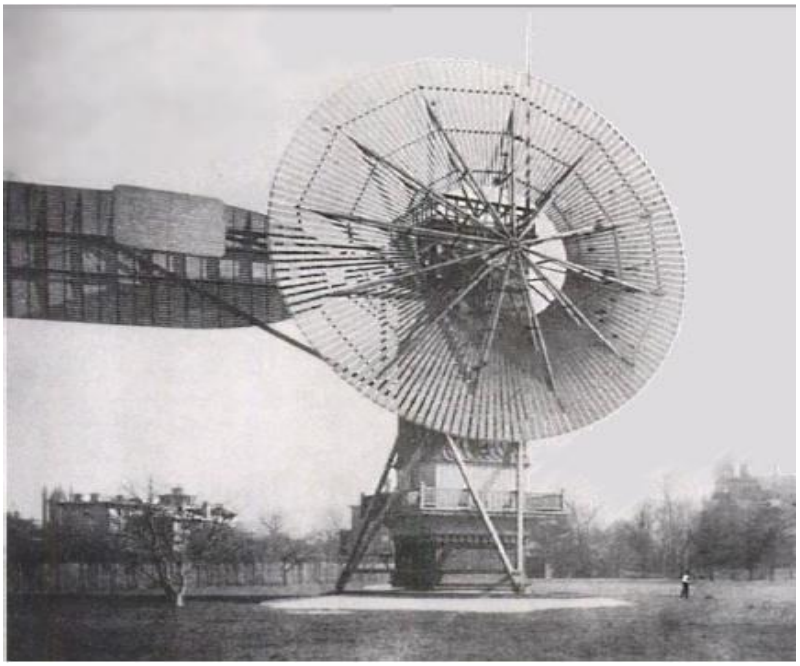

Figure I.1: The first aerodynamic generator.

2. WIND TURBINE TECHNOLOGY

The wind turbine is one of the most important elements in wind energy conversion systems. Over the years, different types of wind turbines have been developed [2], [3]. This section provides an overview of wind turbine technologies, including horizontal/ vertical-axis turbines and fixed/variable-speed turbines.

2.1. HORIZONTAL- AND VERTICAL-AXIS WIND TURBINES

Wind turbines can be categorized based on the orientation of their spin axis into horizontal-axis wind turbines (HAWT) and vertical-axis wind turbines (VAWT) [2],[3]. as shown in Figure I.2.

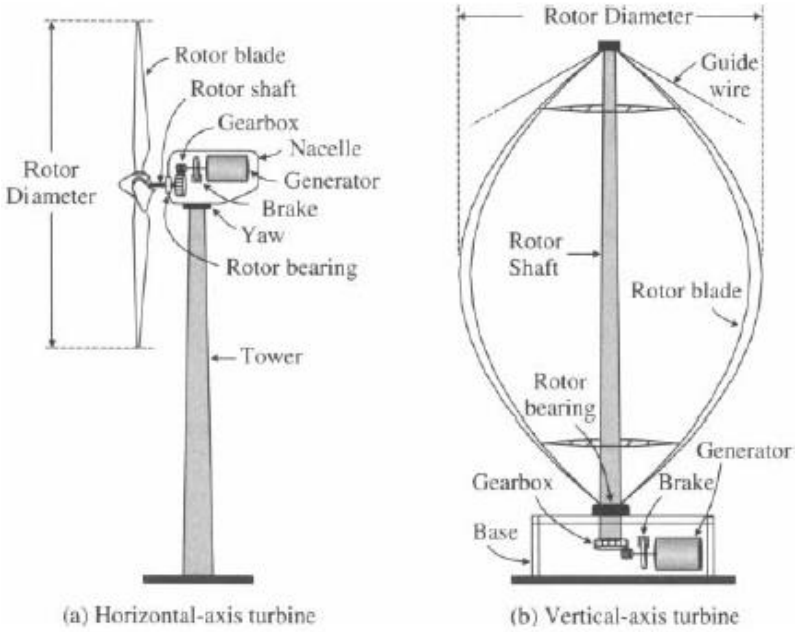

Figure I.2: Horizontal- and vertical-axis wind turbines.

2.1.1. Horizontal-Axis Wind Turbines

The horizontal-axis wind turbine dominates the majority of the wind industry because its efficiency is higher than that of all other types of machines. "Horizontal-axis" means that the turbine's rotating axis is horizontal, or parallel to the horizon. These turbines typically have two- or three-blade rotors, or multi-blade rotors for water pumping. The advantage of the horizontal-axis turbine is that it can generate more electricity for a given amount of wind. However, its drawback appears in the case of turbulent winds due to its mass [4].

2.1.2.Vertical-Axis Wind Turbines

In vertical-axis wind turbines, the orientation of the spin axis is perpendicular to the ground. The turbine rotor uses curved vertically mounted airfoils. The generator and gearbox are normally placed in the base of the turbine on the ground, as shown in Figure l-2b. The rotor blades of the VAWT have a variety of designs with different shapes and number of blades.[3]

2.2. FIXED- AND VARIABLE-SPEED TURBINES

2.2.1. Fixed-Speed Turbines

Fixed-speed wind turbines rotate at almost a constant speed, which is determined by :

- The gear ratio,
- The grid frequency,
- The number of poles of the generator.
- The maximum conversion efficiency can be achieved only at a given wind speed, and the system efficiency degrades at other wind speeds [3].

2.2.2. Variable-Speed Turbines

On the other hand, variable-speed wind turbines can achieve maximum energy conversion efficiency over a wide range of wind speeds. The turbine can continuously adjust its rotational speed according to the wind speed. In doing so, the tip speed ratio, which is the ratio of the blade tip speed to the wind speed, can be kept at an optimal value to achieve the maximum power conversion efficiency at different wind speeds. To make the turbine speed adjustable, the wind turbine generator is normally connected to the utility grid through a power converter system .The converter system enables the control of the speed of the generator that is mechanically coupled to the rotor (blades) of the wind turbine[3].

2.3. STALL CONTROL

The blades are designed to naturally generate aerodynamic turbulence at high wind speeds, which reduces the captured power without the need for control equipment. This method is used in small turbines; it is simple and cost-effective but has low efficiency at low wind speeds.

The stall control technique also offers several advantages [5]:

- ✓ No need for a blade pitch control system.
- ✓ Simpler and less expensive rotor construction.
- ✓ Easier maintenance and improved reliability.

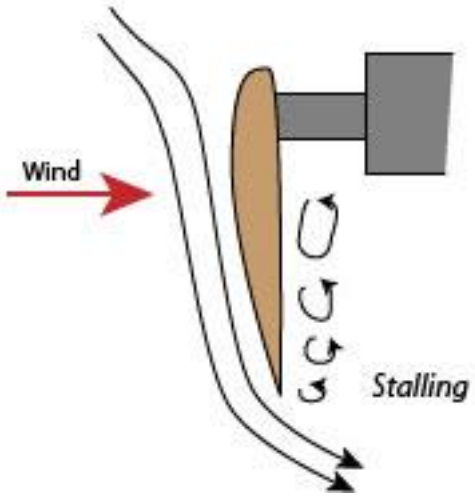

Figure I.3 : Stall Control of Wind Turbine.

2.4. PITCH CONTROL

A mechanical system is used to rotate the blades based on wind speed. At high speeds, the blades are turned away from the wind direction to reduce the captured power. This method is used in large turbines and provides precise control, but it is more expensive and complex.

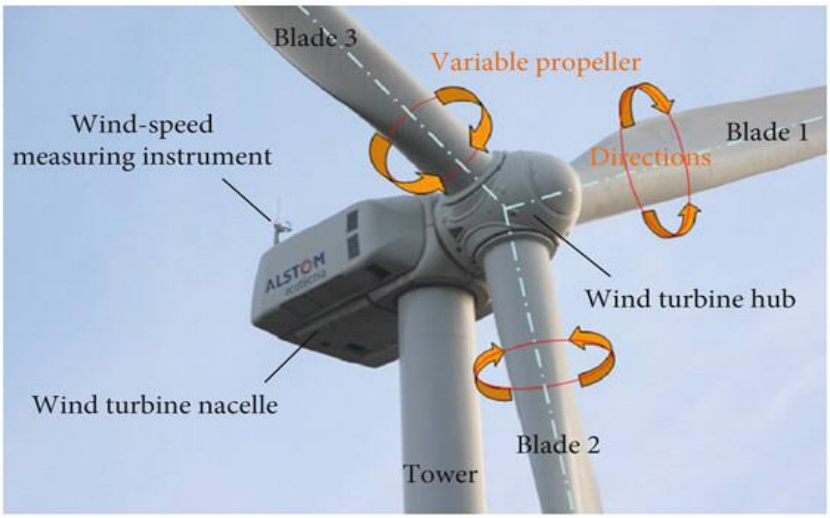

Figure I.4 : Pitch Controller Design of Wind Turbine.

3. WIND TURBINE COMPONENTS

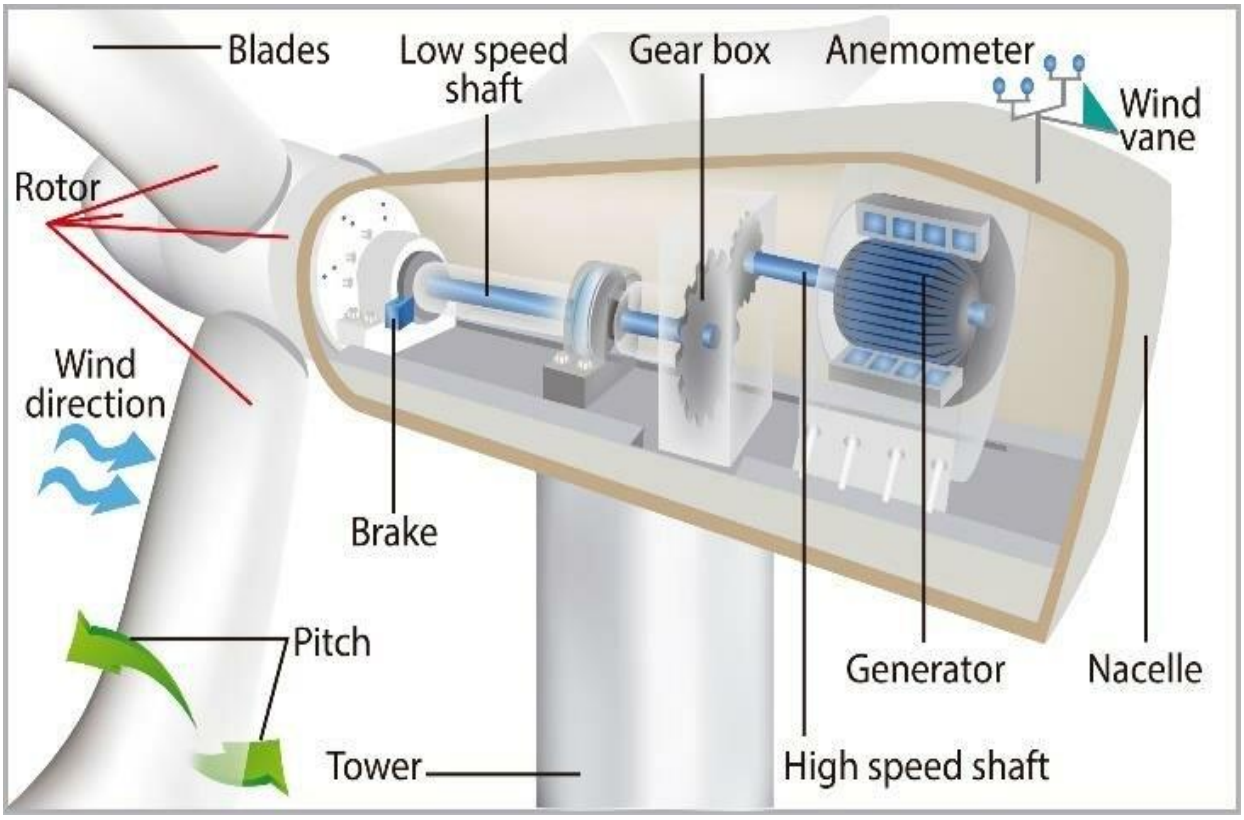

Figure I.5: Main components of a wind turbine.

- Blade
- Gearbox
- Generator
- Nacelle
- Tower
- Rotors
- Anemometer
- Brake(Mechanical)

4. GENERAL DESCRIPTION OF A WIND TURBINE SYSTEM

Basically, the wind's kinetic energy is converted into mechanical energy by the rotor. A gear box transforms the blades' slow rotations (between 18 and 25 per minute) into faster rotations (up to 1,800 per minute) that can power the electric generator. The electric generator converts the mechanical energy into electricity. A transformer transfers the electricity from one circuit to another (eg. the electric grid), modifying its characteristics.

The following figure illustrates the basic principle of operation of a wind turbine system .

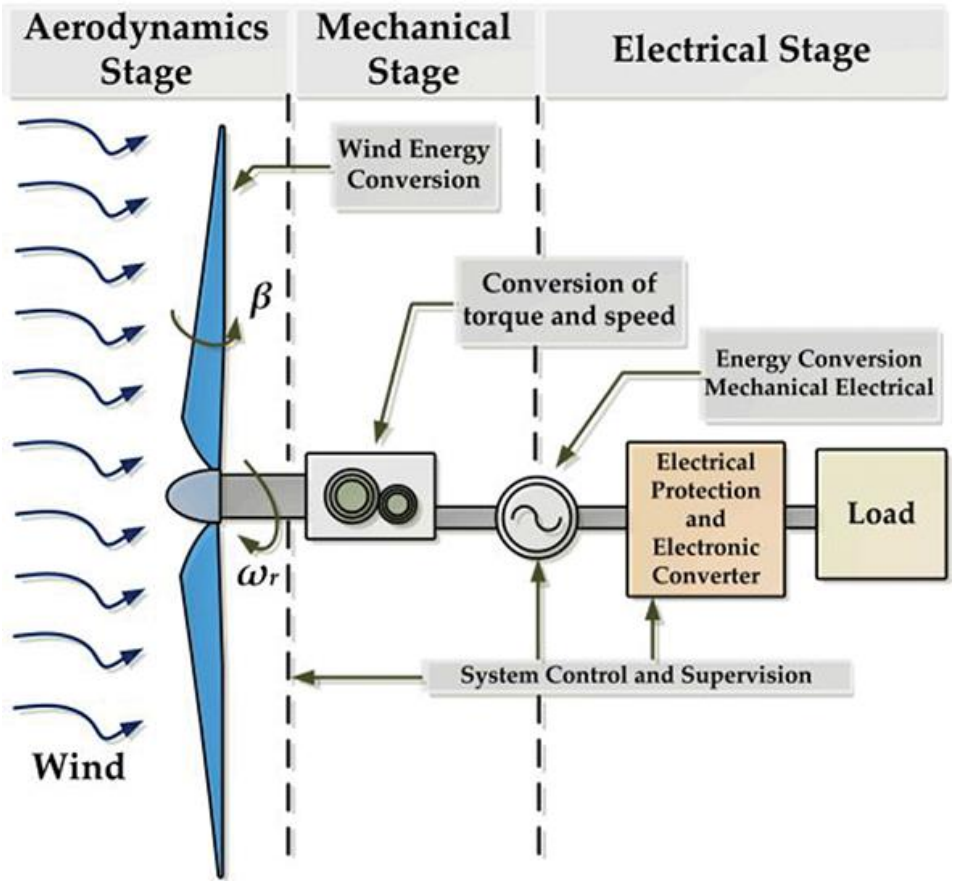

Figure I.6: Basic principle of operation of a wind system.

5. POWER CHARACTERISTIC OF A WIND TURBINE

The power characteristics of a wind turbine are defined by the power curve, which relates the mechanical power of the turbine to the wind speed. The power curve is a wind turbine's certificate of performance that is guaranteed by the manufacturer.A typical power curve is characterized by three wind speeds: cut-in wind speed, rated wind speed, and cut-out wind speed, as described in Figure I.7 [3].

- **The cut-in wind speed**

as the name suggests, is the wind speed at which the turbine starts to operate and deliver power. The blade should be able to capture enough power to compensate for the turbine power losses.

- **The rated wind speed**

is the speed at which the system produces nominal power, which is also the rated output power of the generator.

- **The cut-out wind speed**

is the highest wind speed at which the turbine is allowed to operate before it is shut down. For wind speeds above the cut-out speed, the turbine must be stopped, preventing damage from excessive wind.

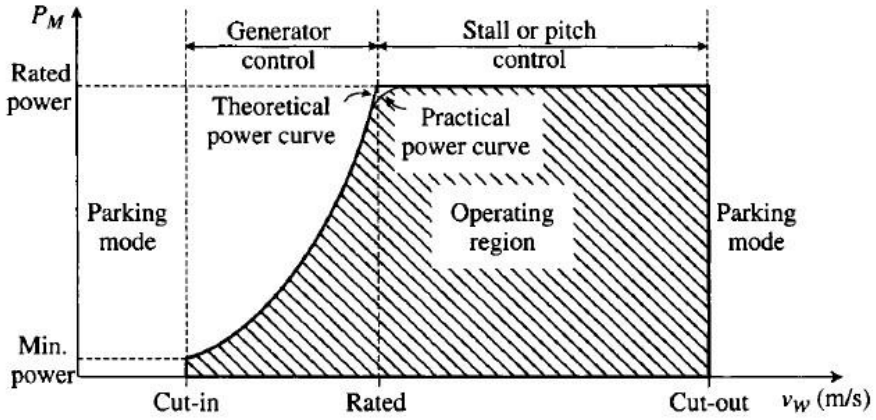

Figure I.7: Qualitative turbine mechanical power versus wind speed curve.

Where :

P_M : is the mechanical power generated by the turbine .
V_w : is the wind speed.

6.AERODYNAMIC POWER CAPTURED BY WIND TURBINE AND POWER COEFFICIENT

Betz's theorem states that the wind velocity V_m over the area S swept by the rotor is assumed to be the average of the free-stream wind velocity V upstream of the turbine and the velocity V_2 downstream of the rotor plane.This is shown in the figure I.8 [5] :

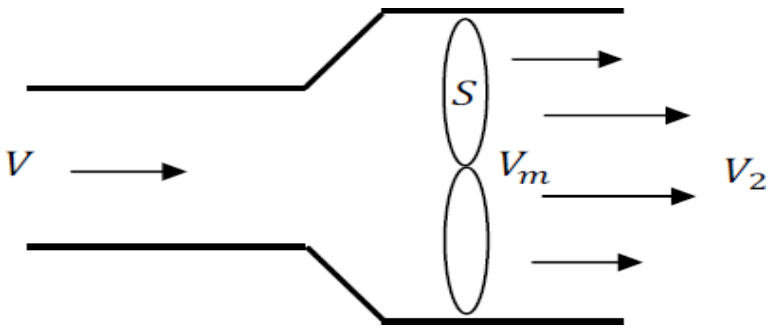

Figure I.8 : Demonstration of Betz's law.

$$V_m = \frac{V + V_2}{2} \quad (I.1)$$

Thus, the mass of air passing through the surface swept by the rotor is given by [5]:

$$m = \frac{1}{2} \rho S (V + V_2) \quad (I.2)$$

Where :

ρ : is the density of air.

V : is the wind speed.

V_m : Medium wind speed.

V_2 : Outlet wind speed.

Moreover, the power extracted from the wind by the turbine, based on Newton's second law, can be expressed by the following equation :

$$P_t = \frac{1}{2} m (V^2 - V_2^2) \quad (I.3)$$

Replacing m by its expression in equation (I.3) we obtain:

$$P_t = \frac{1}{4} \cdot \rho \cdot S \cdot (V^2 - V_2^2) \cdot (V + V_2) \quad (I.4)$$

Now, if we compare this result with the total power of an undisturbed airflow passing through the same surface S, without the interference of the rotor, this power P_w can be expressed as follows [5] :

$$P_w = \frac{1}{2} \cdot \rho \cdot S \cdot V^3 \quad (I.5)$$

The ratio between the power extracted from the wind and the total power theoretically available is defined by [5]:

$$\frac{P_t}{P_w} = \frac{1}{2} \left(1 - \frac{V_2^2}{V^2}\right)\left(1 + \frac{V}{V_2}\right) \quad (I.6)$$

The following figure illustrates the ratio of two powers as a function of the ratio of the two wind speeds downstream and upstream:

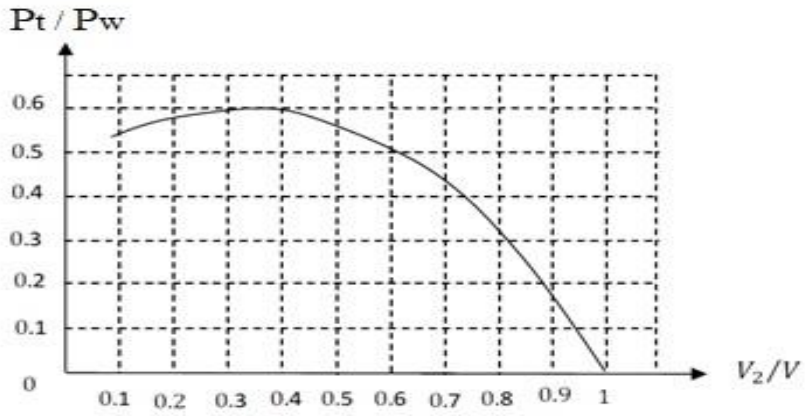

Figure I.9 :Ratio of the two powers as a function of the ratio of the two wind speeds downstream and upstream.

According to figure I.9, it is observed that the function reaches it's maximum when (V_2/V = 1/3), and the maximum value of the wind power that can be extracted is approximately 0.593 of the total power contained in the wind.

However, in practice, the conversion device extracts a power P_t that is lower than the available wind power P_w. Therefore, the power coefficient of the wind turbine is defined by the following relation:

$$C_p = \frac{P_t}{P_w} \tag{I.7}$$

With : $Cp < 1$.

We also write:

$$P_t = C_p P_w \tag{I.8}$$

Replacing P_w by its expression in (I.5), we will have:

$$P_t = \frac{1}{2} C_p S \rho V^3 \tag{I.9}$$

Where $\boldsymbol{P_t}$ represents the power extracted, the power coefficient C_p depends on the rotational speed of the turbine and can be expressed as a function of the tip speed ratio $\boldsymbol{\lambda}$, as follows [5]:

$$C_p = C_p(\lambda) \tag{I.10}$$

$$\lambda = \boldsymbol{\Omega} t \frac{R}{V} \tag{I.11}$$

ΩtR : It is the linear peripheral speed at the tip of the rotor blade.

It is noted that C_p can vary for the same type of turbine depending on the number of blades , although its value remains well below the Betz limit (0.593). For a given turbine, this coefficient may also change according to the pitch angle, which indicates the degree of blade inclination [5].

7.MODELING OF DUAL STAR ASYNCHRONOUS MACHINE(DSAM)

7.1.INTRODUCTION

The modeling of the two-star asynchronous motor (Double Star Asynchronous Motor) is critical in the field of electrical machinery control.These engines are complex systems that combine the advantages of conventional asynchronous engines with advanced dual-file design, making accurate mathematical modeling a prerequisite. There are factors that interfere with this complexity, such as saturation, skin effect and nonlinear phenomena. So here we take some assumptions to facilitate modeling.

7.2.HYPOTESES SYMPOLIQUES

- The asynchronous machine comprises a distribution of windings and a very complex geometry. Therefore, for an analysis taking into account its exact configuration it is necessary to adopt simplifying assumptions [7].
- Unsaturated magnetic circuits are assumed. The relations between flux and current are linear.
- A uniform current density in the conductor section is considered.
- elementary, the skin effect is thus neglected.
- Hysteresis and eddy currents are neglected.
- The stator and rotor windings are symmetrical, and the electromotive force is distributed sine-wave along the periphery of both frames.
- Only the first harmonic of space distribution of magnetotropic force of each phase of the stator and rotor is taken into account. The air gap is of uniform (constant) thickness, the inductances are constant. Mutual inductances are sinusoidal functions of the angle between the axes of the rotor and stator windings.

7.3.MATHEMATICAL MODEL OF DUAL STAR ASYNCHRONOUS MACHINE

In the mathematical description of dual stator asynchronous machine it is assumed that the DSAM machine is considered as an electromechanical system consisting of two three-phase stator windings,

called as stator 1 and stator 2, whose magnetic axes are displaced by γ =30° electrical angle. and the common squirrel-cage rotor winding. The cage rotor winding is replaced by an equivalent three-phase winding. Figure I.10 shows the representation of the stator and rotor windings of dual stator asynchronous machine.

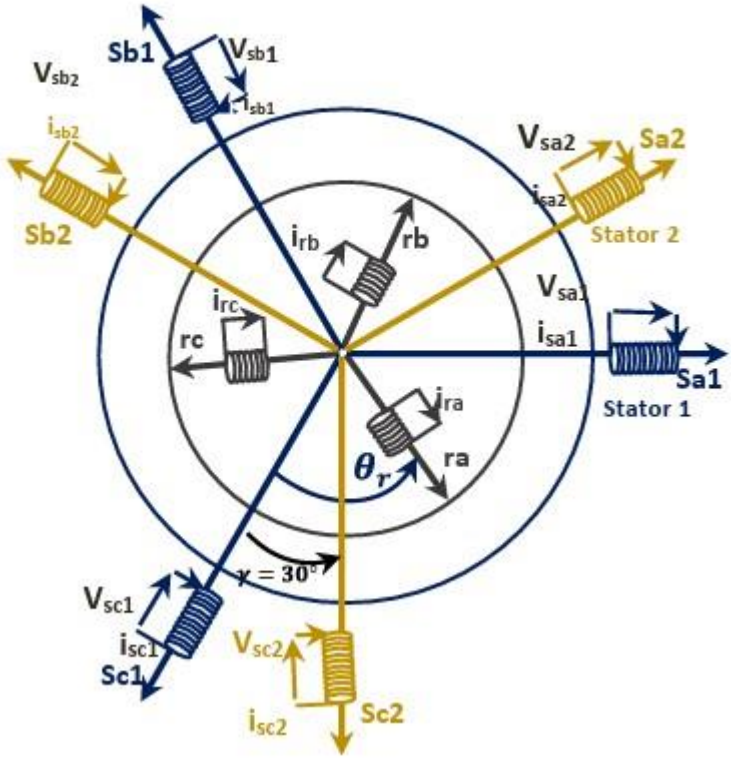

Figure I.10 : Windings scheme of DSIM.

7.4.GENERAL MACHINE EQUATIONS

In the above conditions, the equations of the stator and rotor electrical circuits are presented in the following :

7.4.1.Voltage equations

The electrical equations of the three-phase MAS model are respectively:

For the first stator :

$$[V_{s1}] = [R_{s1}][I_{s1}] + \frac{d}{dt}[\phi_{s1}] \quad \text{(I.12)}$$

For the second stator :

$$[V_{s2}] = [R_{s2}][I_{s2}] + \frac{d}{dt}[\phi_{s2}] \quad \text{(I.13)}$$

For the rotor :

$$0 = [R_r][I_r] + \frac{d}{dt}[\phi_r] \quad \text{(I.14)}$$

Note : The rotor is in short circuit its voltages are zero.

With :

The stator (star 1 and star 2) and rotor voltage, current, and flux vectors equations are defined as follows:

For the first stator:

$$[V_{s1}] = [v_{sa1} \quad v_{sb1} \quad v_{sc1}]^T \quad \text{(I.15)}$$

$$[I_{s1}] = [i_{sa1} \quad i_{sb1} \quad i_{sc1}]^T \quad \text{(I.16)}$$

$$[\phi_{s1}] = [\Phi_{sa1} \; \Phi_{sb1} \; \Phi_{sc1}]^T \quad \text{(I.17)}$$

For the second stator:

$$[V_{s2}] = [v_{sa2} \quad v_{sb2} \quad v_{sc2}]^T \quad \text{(I.18)}$$

$$[I_{s2}] = [i_{sa2} \quad i_{sb2} \quad i_{sc2}]^T \quad \text{(I.19)}$$

$$[\phi_{s2}] = [\Phi_{sa2} \; \Phi_{sb2} \; \Phi_{sc2}]^T \quad \text{(I.20)}$$

For the rotor:

$$[V_r] = [v_{ra} \quad v_{rb} \quad v_{rc}]^T \quad \text{(I.21)}$$

$$[I_r] = [i_{ra} \quad i_{rb} \quad i_{rc}]^T \quad \text{(I.22)}$$

$$[\phi_r] = [\Phi_{ra} \; \Phi_{rb} \; \Phi_{rc}]^T \quad \text{(I.23)}$$

7.4.2.Magnetic equations

The relations between stator and rotor flows and currents are as follows:

For the first stator:

$$[\phi_{s1}] = [L_{s1,s1}][I_{s1}] + [M_{s1,s2}][I_{s2}] + [M_{s1,r}][I_r] \quad \text{(I.24)}$$

For the second stator:

$$[\phi_{s2}] = [M_{s2,s1}]\,[I_{s1}] + [L_{s2,s2}]\,[I_{s2}] + [M_{s2,r}]\,[I_r] \quad \text{(I.25)}$$

For the rotor:

$$[\phi_r] = [M_{r,s1}]\,[I_{s1}] + [M_{r,s2}]\,[I_{s2}] + [L_{r,r}]\,[I_r] \quad \text{(I.26)}$$

$$[L_{s1,s1}] = \begin{bmatrix} L_{s1} + L_{ms} & -L_{ms}/2 & -L_{ms}/2 \\ -L_{ms}/2 & L_{s1} + L_{ms} & -L_{ms}/2 \\ -L_{ms}/2 & -L_{ms}/2 & L_{s1} + L_{ms} \end{bmatrix} \quad \text{(I.27)}$$

$$[L_{s2,s2}] = \begin{bmatrix} L_{s2} + L_{ms} & -L_{ms}/2 & -L_{ms}/2 \\ -L_{ms}/2 & L_{s2} + L_{ms} & -L_{ms}/2 \\ -L_{ms}/2 & -L_{ms}/2 & L_{s2} + L_{ms} \end{bmatrix} \quad \text{(I.28)}$$

$$[L_{r,r}] = \begin{bmatrix} L_r + L_{mr} & -L_{mr}/2 & -L_{mr}/2 \\ -L_{mr}/2 & L_r + L_{mr} & -L_{mr}/2 \\ -L_{mr}/2 & -L_{mr}/2 & L_r + L_{mr} \end{bmatrix} \quad \text{(I.29)}$$

$$[M_{s1,s2}] = L_{ms} \begin{bmatrix} cos\,\alpha & cos\,(\alpha + \frac{2\pi}{3}) & cos\,(\alpha + \frac{4\pi}{3}) \\ cos\,(\alpha + \frac{4\pi}{3}) & cos\,\alpha & cos\,(\alpha + \frac{2\pi}{3}) \\ cos\,(\alpha + \frac{2\pi}{3}) & cos\,(\alpha + \frac{4\pi}{3}) & cos\,\alpha \end{bmatrix} \quad \text{(I.30)}$$

$$[M_{s1,r}] = M_{sr} \begin{bmatrix} cos\,\theta_r & cos\,(\theta_r + \frac{2\pi}{3}) & cos\,(\theta_r + \frac{4\pi}{3}) \\ cos\,(\theta_r + \frac{4\pi}{3}) & cos\,\theta_r & cos\,(\theta_r + \frac{2\pi}{3}) \\ cos\,(\theta_r + \frac{2\pi}{3}) & cos\,(\theta_r + \frac{4\pi}{3}) & cos\,\theta_r \end{bmatrix} \quad \text{(I.31)}$$

$$[M_{s2,r}] = M_{sr} \begin{bmatrix} cos\,(\theta_r - \alpha) & cos\,((\theta_r - \alpha) + \frac{2\pi}{3}) & cos\,((\theta_r - \alpha) + \frac{4\pi}{3}) \\ cos\,((\theta_r - \alpha) + \frac{4\pi}{3}) & cos\,(\theta_r - \alpha) & cos\,((\theta_r - \alpha) + \frac{2\pi}{3}) \\ cos\,((\theta_r - \alpha) + \frac{2\pi}{3}) & cos\,((\theta_r - \alpha) + \frac{4\pi}{3}) & cos\,(\theta_r - \alpha) \end{bmatrix} \quad \text{(I.32)}$$

With :

$[M_{s1,s2}] = [M_{s2,s1}]^T$; $[M_{s1,r}] = [M_{r,s1}]^T$;$[M_{s2,r}] = [M_{r,s2}]^T$

7.4.3.Mechanical equation

The fundamental equation of the machine movement is given by:

$$\frac{d}{dt}\Omega_m = \frac{1}{J}(T_{em} - T_r - K_f\Omega_m) \quad \text{(I.33)}$$

$$\frac{d}{dt}\theta_m = \Omega_m \quad \text{(I.34)}$$

$with$:

- J : Moment of inertia.
- Ω : Rotation speed of the rotor.
- T_r : Torque resistant.
- T_{em} : Electromagnetic torque.
- K_f ; Coefficient of friction.

7.4.4. Electromagnetic torque expression

The electromagnetic torque is expressed by the partial derivative of storage of electromagnetic energy relative to the geometric angle of rotation of the rotor.

$$T_{em} = \frac{\partial w}{\partial \theta_{geo}} = P\frac{\partial w}{\partial \theta_{ele}} \quad \text{(I.35)}$$

With :

$$w = \frac{1}{2}([i_{s1}]^t[\phi_{s1}] + [i_{s1}]^t[\phi_{s2}] + [i_r]^t[\phi_r])$$

We can extract the torque electromagnetic and write it like that:

$$T_{em} = \frac{p}{2}\left([i_{s1}]\ \frac{d}{d\theta_r}[L_{s1r}]\ [i_r]^t + [i_{s2}]\ \frac{d}{d\theta_r}[L_{s2r}]\ [i_r]^t\right) \quad \text{(I.36)}$$

If we look at the terms of the electrical tension of this machine, it's related to the electric current, which explains to us that the coefficients will not be fixed and will be complex, so we use a conversion that enables us to simplify those transactions and move from the triple system to the binary system, which is called Park conversion:

8. MODELING OF THE ASYNCHRONOUS MACHINE IN THE TWO-PHASE LANDMARK

The model of the machine in the three-phase reference frame is very complex, and two-phase transformation is used to simplify it [8]. Physically it can be explained by a transformation of three windings into only two windings as shown in Figure I.11 This simplification should reduce the order of the system and eliminate the dependence on the position of the rotor, that is to say, obtain a model characterized by a constant coefficients equation system.

8.1.PARK TRANSFORMATION

The Park transformation involves converting the stator three-phase winding system with axes A, B, and C into an equivalent two-winding system followed by a rotation, creating the same magnetomotive force [9]. It allows for a transition from the reference frames (A, B, C) to (β, α, o), and then to (d, q, o). The reference frame (β, α, o) remains fixed relative to (A, B, C), whereas the reference frame (d, q, o) is mobile. The angle between these two frames is known as the Park transformation angle or Park angle.

In this context, "d" refers to the direct axis and "q" refers to the quadrature axis. The clockwise rotation is introduced by the following matrix:

$$[P] = \frac{2}{3}\begin{bmatrix} cos\,\theta & cos\left(\theta + \frac{2\pi}{3}\right) & cos\left(\theta + \frac{4\pi}{3}\right) \\ -sin(\theta) & -sin\left(\theta + \frac{2\pi}{3}\right) & -sin\left(\theta + \frac{4\pi}{3}\right) \\ 1/2 & 1/2 & 1/2 \end{bmatrix} \quad \text{(I.37)}$$

The figure I.11 shows the principle of park transformation :

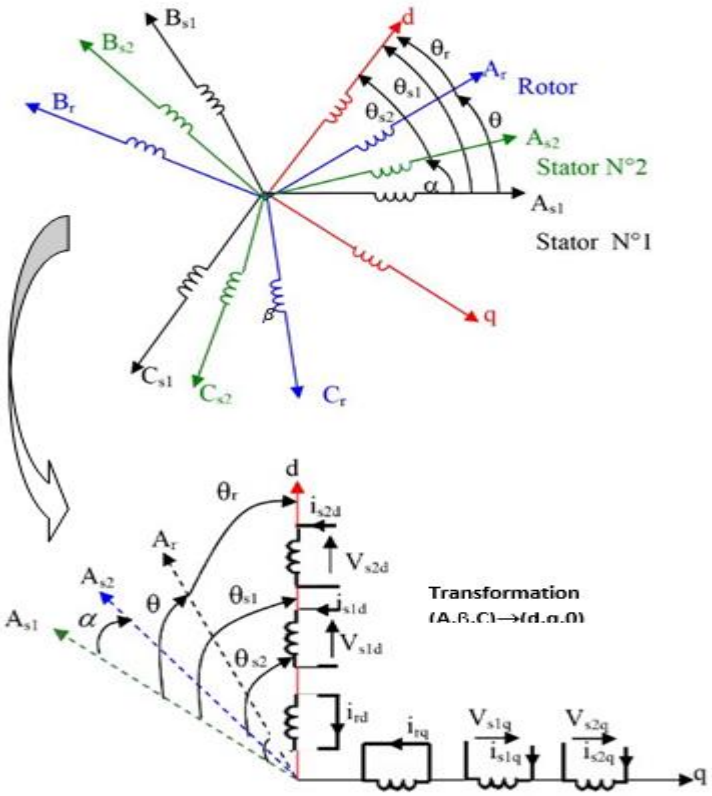

Figure I.11 : Presentation of the passages in the principle of the transformation of the park.

General inverse Park matrix:

$$[P(\theta)]^{-1} = \sqrt{\frac{2}{3}} \begin{pmatrix} \cos(\theta) & -\sin(\theta) & \frac{1}{\sqrt{2}} \\ \cos(\theta - \frac{2\pi}{3}) & \sin(\theta - \frac{2\pi}{3}) & \frac{1}{\sqrt{2}} \\ \cos(\theta + \frac{2\pi}{3}) & -\sin(\theta + \frac{2\pi}{3}) & \frac{1}{\sqrt{2}} \end{pmatrix} \quad \text{(I.38)}$$

The general Park matrix :

$[G_{dqo}]=[P(\theta)].[G_{abc}]$

$[G_{abc}]=[P(\theta)]^{-1}.[G_{dqo}]$

With :

- G_{dqo}: two-phase quantities in the frame of reference (d,q).
- G_{abc}: Balanced three-phase quantities.

with :

$$\theta = \int_0^t \omega_{coor}\, dt$$

θ : angle between two-phase and three-phase axis systems.

ω_{coor} : angular speed of rotation of the two-phase axis system relative to the three-phase axis system.

By converting Park on the machine we will see how it becomes the equations of both current and tension and flow which will become dropped on only two axes .

8.1.1.Equation of voltage

For stator N°1
$$\begin{cases} V_{ds1} = R_s i_{ds1} + \frac{d\phi_{ds1}}{dt} - \omega_s \phi_{qs1} \\ V_{qs1} = R_s i_{qs1} + \frac{d\phi_{qs1}}{dt} + \omega_s \phi_{ds1} \end{cases} \quad \text{(I.39)}$$

For stator N°2
$$\begin{cases} V_{ds2} = R_s i_{ds2} + \frac{d\phi_{ds1}}{dt} - \omega_s \phi_{qs2} \\ V_{qs2} = R_s i_{qs2} + \frac{d\phi_{qs1}}{dt} + \omega_s \phi_{ds2} \end{cases}$$

For rotor
$$\begin{cases} 0 = R_r i_{dr} + \frac{d\phi_{dr}}{dt} + (\omega_s - \omega_r)\, \phi_{qr} \\ 0 = R_r i_{qr} + \frac{d\phi_{qr}}{dt} + (\omega_s - \omega_r)\, \phi_{dr} \end{cases} \quad \text{(I.40)}$$

8.1.2.Equation of flux

As for the application of Park transformation on the voltage equations, we apply this transformation on the flux equations, we obtain [10]:

$$\phi_{ds1} = L_{s1} I_{ds1} + L_m(i_{ds1} + i_{ds2} + i_{dr}) \quad \text{(I.41)}$$

$$\phi_{qs1} = L_{s1} I_{qs1} + L_m(i_{qs1} + i_{qs2} + i_{qr}) \quad \text{(I.42)}$$

$$\phi_{ds2} = L_{s2} I_{ds2} + L_m(i_{ds1} + i_{ds2} + i_{dr}) \quad \text{(I.43)}$$

$$\phi_{qs2} = L_{s2} I_{qs2} + L_m(i_{qs1} + i_{qs2} + i_{qr}) \quad \text{(I.44)}$$

$$\phi_{dr} = L_r I_{dr} + L_m(i_{ds1} + i_{ds2} + i_{dr}) \quad \text{(I.45)}$$

$$\phi_{qr} = L_r I_{qr} + L_m(i_{ds1} + i_{ds2} + i_{dr}) \quad \text{(I.46)}$$

8.1.3. Mechanical equation

The expression of the electromagnetic torque can be obtained using a power balance. By using the fluxes and currents from the system of equations of voltage we can have several expressions of the torque, all equal[9]:

$$P = [V_s]^t[I_s] = V_{sa1}I_{sa1} + V_{sb1}I_{sb1} + V_{sc1}I_{sc1} + V_{sa2}I_{sa2} + V_{sb2}I_{sb2} + V_{sc2}I_{sc2} \quad (I.47)$$

Taking into account that the Park transform conserves instantaneous power, the DSAM power equation can be expressed as:

$$P=(V_{ds1})I_{ds1} + (V_{qs1})I_{qs1} + (V_{ds2})I_{ds2} + (V_{qs2})I_{qs2} \quad (I.48)$$

Replacing the voltages and currents of axes (d, q) in the system of equations (I.38) by their expressions in equation of voltage we find the following expression for the instantaneous absorbed power [10] :

$$\begin{aligned} P_{abs} &= [R_{s1}i_{ds1}^2 + R_{s1}i_{qs1}^2 + R_{s2}i_{ds2}^2 + R_{s2}i_{qs2}^2] \\ &+ [\omega_s(\Phi_{ds1}i_{qs1} - \Phi_{qs1}i_{ds1} + \Phi_{ds2}i_{qs2} - \Phi_{qs2}i_{ds2})] \\ &+ \frac{d\phi_{ds1}}{dt}i_{ds1} + \frac{d\phi_{qs1}}{dt}i_{qs1} + \frac{d\phi_{ds2}}{dt}i_{ds2} + \frac{d\phi_{qs2}}{dt}i_{qs2} \end{aligned} \quad (I.49)$$

It should be noted that the equation for instantaneous generated power consists of three terms[9]:

- The first term represents the joule losses at the stator.
- The second term represents the stored electromagnetic power.
- The third term represents the electrical power transformed to mechanical power.

Electromagnetic potential and torque can be written in universal form :

$P_{em} = \Omega_s T_{em}$

With :

Ω_s : The mechanical rotation speed of the rotor.

Tem : The electromagnetic torque.

In the expression for absorbed power (I.49) we have the second term which represents the electromagnetic power[10] :

$$P_{em} = \omega coor\ (\phi_{ds1} i_{qs1} - \phi_{qs1} i_{ds1} + \phi_{ds2} i_{qs2} - \phi_{qs2} i_{ds2}) \quad (I.50)$$

8.1.4.Electromagnetic Torque

From equation (I.51) it is clear that the electromagnetic torque is of the following form :

$$T_{em} = P(\phi_{ds1} i_{qs1} + \phi_{ds2} i_{qs2} - \phi_{qs1} i_{ds1} - \phi_{qs2} i_{ds2}) \quad (I.51)$$

P: Is the number of pole pairs of the machine

9.REFERENCE CHOICE

To study the theory of transient regimes of the double star asynchronous machine, three systems of coordinate axes of the axis plane can be used (d,q).

9.1. STATOR REFERENCE FRAME

In this frame of reference, the axes (d, q) are stationary relative to the stator ($\omega_{coor} = 0$). In this case, the phases As1 and d coincide. This frame of reference is best suited for working with instantaneous quantities and has the advantage of not requiring a transformation to the real system.The use of this system makes it possible to study the starting and braking regimes of alternating current machines [11], [10],[13].

9.2. ROTOR REFERENCE FRAME

In this frame of reference, the axes (d,q) are stationary relative to the rotor rotating at a speed ω_r so ($\omega_{coor} = \omega_r$) .

The use of this reference framework allows the study of transient regimes in synchronous and asynchronous AC machines with non-symmetrical connection of the rotor circuits.

9.3. ROTATING FIELD REFERENCE FRAME

In this frame of reference, the axes (q, d) are stationary relative to the electromagnetic field created by the two stars of the stator ($\omega_{coor} = \omega_s$)

This reference system is generally used in order to be able to apply a speed, torque, etc. command since the quantities in this reference system are continuous[12],[16].

10.MACHINE MODEL

In our work, we use the rotating field-related reference frame for modeling and controlling the DSAM. In this case, the DSAM model becomes :

$$\begin{cases} V_{ds1} = R_s i_{ds1} + \frac{d\phi_{ds1}}{dt} - \omega_s \phi_{qs1} \\ V_{qs1} = R_s i_{qs1} + \frac{d\phi_{qs1}}{dt} - \omega_s \phi_{ds1} \\ V_{ds2} = R_s i_{ds2} + \frac{d\phi_{ds1}}{dt} - \omega_s \phi_{qs2} \\ V_{qs2} = R_s i_{qs2} + \frac{d\phi_{qs1}}{dt} - \omega_s \phi_{ds2} \\ 0 = R_r i_{dr} + \frac{d\phi_{dr}}{dt} - (\omega_s - \omega_r)\, \phi_{qr} \\ 0 = R_r i_{qr} + \frac{d\phi_{qr}}{dt} + (\omega_s - \omega_r)\, \phi_{dr} \end{cases} \quad \text{(I.51)}$$

11.FORMATTING AN EQUATION OF STATE

Since the representation of the DSAM equation of state is to represent the machine model in a (d,q) reference frame, the voltage equation can be rewritten as follows [14]:

$$\frac{dx}{dt} = AX + BU \quad \text{(I.52)}$$

This requires that :

$$\frac{d}{dt}[\phi] = A.[\phi] + B.[V] \quad \text{(I.53)}$$

In the system modeling, magnetic fluxes are integrated into the state vector to describe its dynamic behavior. Stator voltages, having the same dimension as the control vector, are introduced into the input vector. On this basis, matrices A and B must be constructed from the system equations, in order to formalize the state model allowing the analysis and control of the process.

In the following, the state and input vectors are chosen: [14]

$$X = \begin{bmatrix} \Phi_{ds1} \\ \Phi_{ds2} \\ \Phi_{qs1} \\ \Phi_{qs2} \\ \Phi_{dr} \\ \Phi_{qr} \end{bmatrix} \quad \text{(I.54)} \qquad V = \begin{bmatrix} V_{ds1} \\ V_{ds2} \\ V_{qs1} \\ V_{qs2} \\ 0 \\ 0 \end{bmatrix} \quad \text{(I.55)}$$

The two expressions of the magnetizing fluxes as a function of the stator and rotor currents are expressed by [15]:

For the stators :

$$\phi_{ds1} = L_{s1} i_{ds1} + \phi_{md}$$

$$\phi_{qs1} = L_{s1} i_{qs1} + \phi_{mq} \quad \text{(I.56)}$$

$$\phi_{ds2} = L_{s2} i_{ds2} + \phi_{md}$$

$$\phi_{qs2} = L_{s2} i_{qs2} + \phi_{mq}$$

For the rotor :

$$\phi_{dr} = L_r i_{qr} + \phi_{md} \quad \text{(I.57)}$$

$$\phi_{qr} = L_r i_{qr} + \phi_{mq}$$

Then, the expressions for currents can be expressed as follows:

Stators:

$$i_{ds1} = (\phi_{ds1} - \phi_{md}) / L_{s1}$$

$$i_{qs1} = (\phi_{qs1} - \phi_{mq}) / L_{s1} \quad \text{(I.58)}$$

$$i_{ds2} = (\phi_{ds2} - \phi_{md}) / L_{s2}$$

$$i_{qs2} = (\phi_{qs2} - \phi_{mq}) / L_{s2}$$

Rotor :

$$i_{dr} = (\phi_{dr} - \phi_{md}) / L_r \quad \text{(I.59)}$$

$$i_{qr} = (\phi_{qr} - \phi_{mq}) / L_r$$

We can obtain other expressions for the instantaneous torque by using the stator flux expressions and substituting the fluxes given by (I.45) and (I.46) into (I.40), resulting in:

$$T_{em} = p L_m \left[i_{qs1} + i_{qs2} \right) i_{dr} - (i_{ds1} + i_{ds2}) i_{qr} \quad \text{(I.60)}$$

Furthermore, from the rotor flux equations (φ_{dr} and φ_{qr}) expressed by equations flux we derive the expressions for the rotor currents as follows :

$$i_{dr} = \frac{1}{L_m + L_r} [\phi_{dr} - L_m(i_{ds1} + i_{ds2})] \quad \text{(I.61)}$$

$$i_{qr} = \frac{1}{L_m + L_r} [\phi_{qr} - L_m(i_{qs1} + i_{qs2})] \quad \text{(I.62)}$$

By substituting equations (I.62) and (I.63) into equation (I.61), the electromagnetic torque expression in terms of stator currents and rotor fluxes in the Park reference frame (d,q) is obtained as follows:

$$T_{em} = p\frac{Lm}{Lm+Lr}\left[i_{qs1} + i_{qs2}\right)\phi_{dr} - \left(i_{ds1} + i_{ds2}\right)\phi_{qr}] \quad \text{(I.63)}$$

Thus, the state-space form is given by:

$$\begin{aligned}
\frac{d}{dt}\phi_{ds1} &= V_{ds1} + \omega_s\phi_{qs1} + \frac{L_a-L_{s1}}{Ts1Ls1}\phi_{ds1} + \frac{L_a}{Ts1Ls1}\phi_{ds2} + \frac{L_a}{T_{s1}L_r}\phi_{dr} \\
\frac{d}{dt}\phi_{qs1} &= V_{qs1} - \omega_s\phi_{ds1} + \frac{L_a-L_{s1}}{T_{s1}L_{s1}}\phi_{qs1} + \frac{L_a}{T_{s1}L_{s2}}\phi_{qs2} + \frac{L_a}{T_{s1}L_r}\phi_{qr} \\
\frac{d}{dt}\phi_{ds2} &= V_{ds2} + \frac{L_a}{T_{s2}L_{s1}}\phi_{ds1} + \frac{L_a-L_{s2}}{T_{s2}L_{s2}}\phi_{ds2} + \omega_s\phi_{qs2} + \frac{L_a}{T_{s2}L_r}\phi_{dr} \\
\frac{d}{dt}\phi_{qs2} &= V_{qs2} + \frac{L_a}{T_{s2}L_{s1}}\phi_{qs1} - \omega_s\phi_{ds2} + \frac{L_a-L_{s2}}{T_{s2}L_{s2}}\phi_{qs2} + \frac{L_a}{T_{s2}L_r}\phi_{qr} \\
\frac{d}{dt}\phi_{dr} &= \frac{L_a}{T_rL_{s1}}\phi_{ds1} + \frac{L_a}{T_rL_{s2}}\phi_{ds2} + \frac{L_a-L_r}{T_rL_r}\phi_{dr} + \omega_{gl}\phi_{qr} \\
\frac{d}{dt}\phi_{qr} &= \frac{L_a}{T_rL_{s1}}\phi_{qs1} + \frac{L_a}{T_rL_{s2}}\phi_{qs2} + \frac{L_a-L_r}{T_rL_r}\phi_{qr} - \omega_{gl}\phi_{dr}
\end{aligned} \quad \text{(I.64)}$$

The general form of the state equation is written as follows:

$$\dot{X} = AX + BU \quad \text{(I.65)}$$

With :

$$\begin{cases} [X] = \left[\phi_{ds1}\ \ \phi_{ds2}\ \phi_{qs1}\ \phi_{qs2}\ \phi_{dr}\ \phi_{qr}\right]^T \\ [U] = \left[\ V_{ds1}\ V_{qs1}\ V_{ds2}\ V_{qs2}\right] \end{cases}$$

$$A=\begin{bmatrix}
\frac{L_a-L_{s1}}{T_{s1}L_{s1}} & \omega_s & \frac{L_a}{T_{s1}L_{s2}} & 0 & \frac{L_a}{T_{s1}L_r} & 0 \\
-\omega_s & \frac{L_a-L_{s1}}{T_{s1}L_{s1}} & 0 & \frac{L_a}{T_{s1}L_{s1}} & 0 & \frac{L_a}{T_{s1}L_r} \\
\frac{L_a}{T_{s2}L_{s1}} & 0 & \frac{L_a-L_{s2}}{T_{s2}L_{s2}} & \omega_s & \frac{L_a}{T_{s2}L_r} & 0 \\
0 & \frac{L_a}{T_{s2}L_{s1}} & -\omega_s & \frac{L_a-L_{s2}}{T_{s2}L_{s2}} & 0 & \frac{L_a}{T_{s2}L_r} \\
\frac{L_a}{T_rL_{s1}} & 0 & \frac{L_a}{T_rL_{s2}} & 0 & \frac{L_a-L_r}{T_rL_r} & \omega_{sl} \\
0 & \frac{L_a}{T_rL_{s1}} & 0 & \frac{L_a}{T_rL_{s2}} & -\omega_{sl} & \frac{L_a-L_r}{T_rL_r}
\end{bmatrix} \quad \text{(I.66)}$$

$$B = \begin{bmatrix} 1 & 0 & 0 & 0 \\ 0 & 1 & 0 & 0 \\ 0 & 0 & 1 & 0 \\ 0 & 0 & 0 & 1 \\ 0 & 0 & 0 & 0 \\ 0 & 0 & 0 & 0 \end{bmatrix} \quad \text{(I.67)}$$

With :

$T_{s1} = \frac{L_{s1}}{R_{s1}}$: Stator time constant of the first star.

$T_{s2} = \frac{L_{s2}}{R_{s2}}$: Stator time constant of the second star.

$T_r = \frac{L_r}{R_r}$: Stator time constant of the rotor.

12.POWER SUPPLY AND CONTROL OF DSAM BY PWM

12.1.INTRODUCTION

Pulse Width Modulation (PWM) is considered one of the most important control strategies used in power electronics. It allows the generation of voltage signals with variable effective values using pulses of fixed frequency and variable width.
This technique is widely applied in controlling the speed and torque of electric machines, particularly asynchronous machine, by regulating the voltage and frequency supplied to the motor.

This inverter allows the generation of voltage waves for the electrical machine with variable amplitude and frequency from a conventional electrical grid with a voltage of 220/380 V and a frequency of 50 Hz [17].

When applied to double-star asynchronous machine, PWM enables the distribution of voltage and current across two stator winding groups, which helps reduce harmonics and improve dynamic performance. It also allows operation at higher frequencies using lower-rated electronic components. This distribution contributes to enhancing efficiency and achieving precise control of the machine operation under various load conditions.

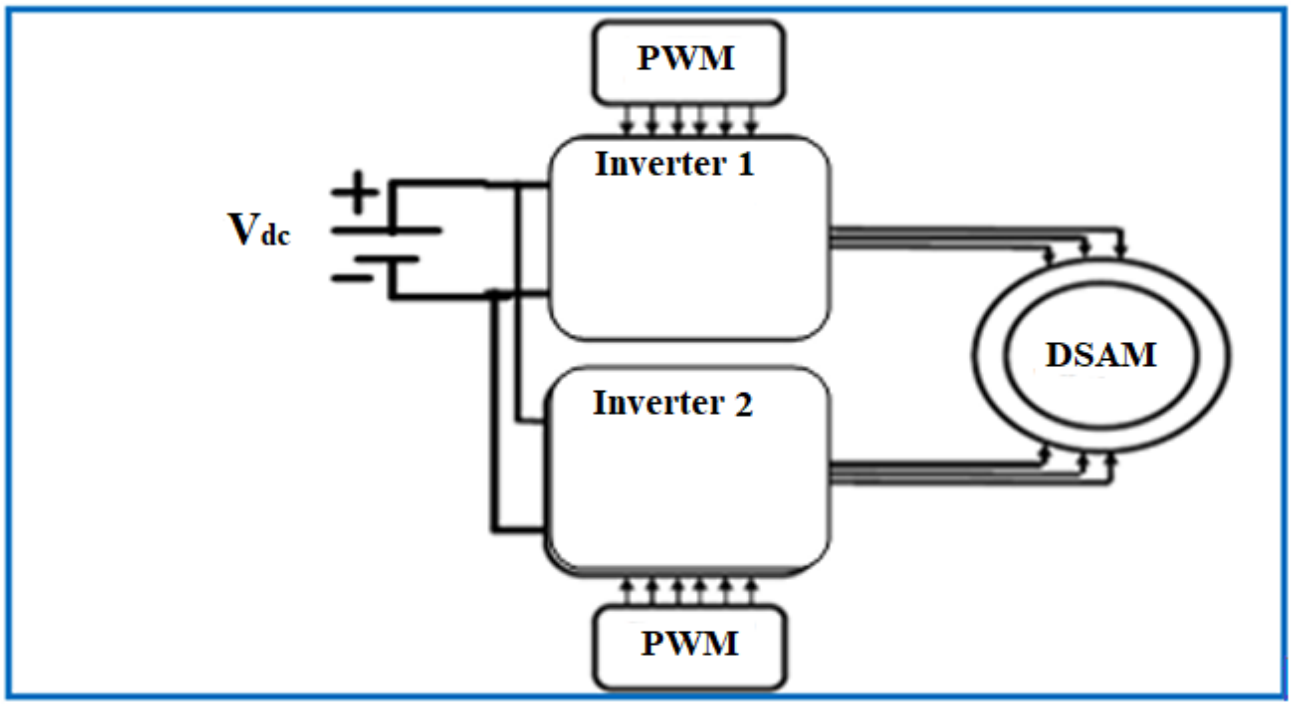

Figure I.12 : Power supply of the double star asynchronous machine.

12.2.MODELING OF THE PWM INVERTER

The structural diagram of such a three-phase two-level inverter and its load is illustrated in Figure I.13. Each transistor-diode group assembled in parallel forms a double-controlled switch (on opening and on closing) whose state appears complementary to that associated with it, thus forming a switching arm [27],[28].

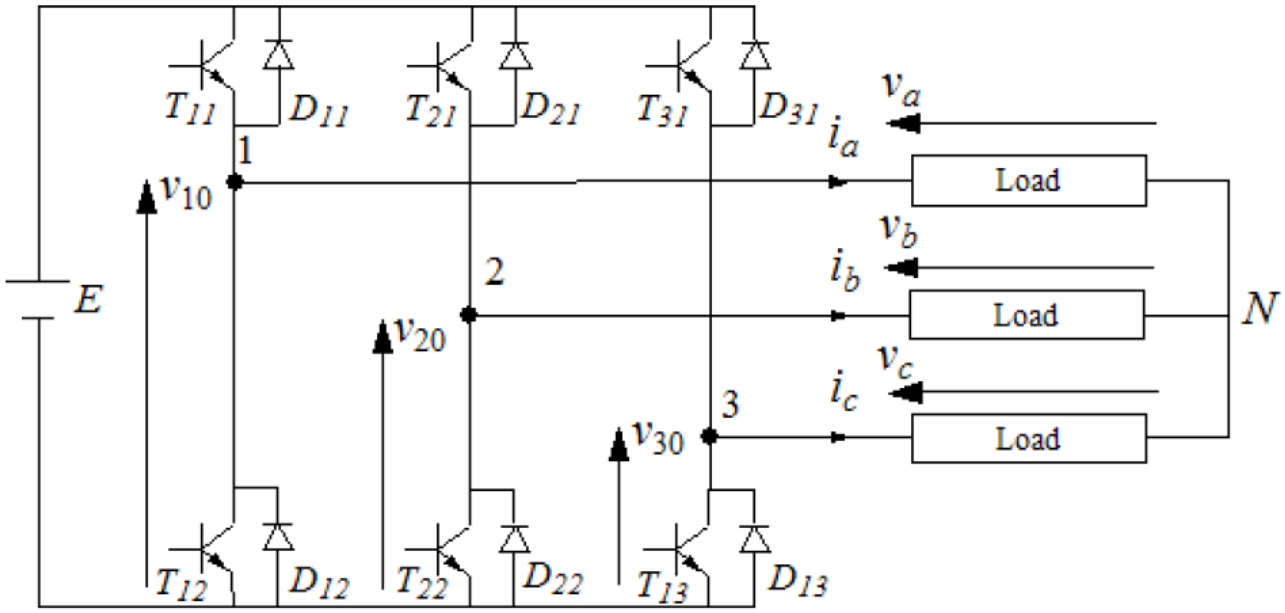

Figure I.13 : Three-phase inverter associated with the DSIM.

We have : $\left.\begin{matrix}\mathbf{i_a}\\ \mathbf{i_b}\\ \mathbf{i_c}\end{matrix}\right\}$ are the phase voltages measured relative to the neutral N of the symmetrical three-phase load. (eg .The stator windings of the first star of the DSAM).

$$V_{10} - V_a + V_b - V_{20} = 0 \tag{I.68}$$

$$V_{10} - V_a + V_c - V_{30} = 0 \tag{I.69}$$

We add equation (I.68) to equation (I.69), we obtain :

$$2V_{10} - 2V_a + V_b + V_c - V_{20} - V_{30} = 0 \tag{I.70}$$

The load is isolated and symmetrical,that main The sum of the currents (i_a, i_b, i_c) must be zero,and the same applies to the phase voltages ($V_a + V_b + V_c = 0$),that main :Va = − (Vb + Vc) , Therefore, in equation (I.71) we get **:**

$$\begin{aligned} V_a &= 1/3(\ 2V_{10} - V_{20} - V_{30}) \\ V_b &= 1/3(-V_{10} + 2V_{20} - V_{30}) \\ V_c &= 1/3(-V_{10} - V_{20} + 2V_{30}) \end{aligned} \tag{I.71}$$

We have two states of the inverter K_{ij}, either closed or open. The branch voltages V_{j0} can be equal to E or 0. We introduce other variables F1,F2,F3 for the first inverter and F4,F5,F6 for the second.

Which take 1 (closed) or 0 (blocked) for switches K_{i1}, respectively.

The power supply of the first inverter is :

$$\begin{bmatrix} V_{as1} \\ V_{bs1} \\ V_{cs1} \end{bmatrix} = \frac{E}{3} \begin{bmatrix} 2 & -1 & -1 \\ -1 & 2 & -1 \\ -1 & -1 & 2 \end{bmatrix} \begin{bmatrix} F_1 \\ F_2 \\ F_3 \end{bmatrix} \tag{I.72}$$

The power supply of the second inverter is :

$$\begin{bmatrix} V_{as2} \\ V_{bs2} \\ V_{cs2} \end{bmatrix} = \frac{E}{3} \begin{bmatrix} 2 & -1 & -1 \\ -1 & 2 & -1 \\ -1 & -1 & 2 \end{bmatrix} \begin{bmatrix} F_4 \\ F_5 \\ F_6 \end{bmatrix} \tag{I.73}$$

12.3. PWM CONTROL STRATEGY

The real-time determination of the switching instants (turn-on and turn-off) of power electronic switches in converters is commonly achieved using Pulse Width Modulation (PWM) techniques, particularly the sinusoidal-triangular modulation method. This approach is based on the comparison between a low-frequency sinusoidal reference signal (modulating wave), which represents the desired output waveform, and a high-frequency triangular carrier signal. The intersections of these two signals define the precise switching instants [18]. This strategy can be implemented using either analog or digital control electronics, and it enables the generation of control signals required for switch operation [19]. The switching frequency is determined by the carrier signal, while two key parameters characterize the modulation: the modulation index mmm, defined as the ratio of the carrier frequency f_p to the modulating frequency f_r, and the voltage regulation ratio r, defined as the ratio of the reference signal amplitude to the peak amplitude of the carrier U_{pm} [20]. When non-sinusoidal modulation functions are employed, the converter's performance can be significantly enhanced by increasing the fundamental component and the harmonic content of the output voltage. However, such methods are often complex and may not be feasible for real-time control applications [21]. The six reference signals for the two inverters are given by[22],[23],[24] :

$$V_{ks1ref} = V_m \sin[2\pi f t - 2(j-1)\frac{\pi}{3}] \tag{I.74}$$

$$V_{ks1ref} = V_m \sin\left[2\pi f t - 2(j-1)\frac{\pi}{3}\right] - \alpha \tag{I.75}$$

With :

$k = a, b, c$

$j = 1\ , 2, 3\ .$

$$V_p(t) = \begin{cases} V_{pm}\left[4\frac{t}{T_p} - 1\right] & if \quad 0 \le t \le \frac{T_p}{2} \\ V_{pm}\left[-4\frac{t}{T_p} + 3\right] & if \quad \frac{T_p}{2} \le t \le T_p \end{cases} \tag{I.76}$$

With :

T_p: The modulation period.

V_{pm}: The peak value of the modulation waveform.

In this method we have two important elements: Modulation index (m) and Adjustment coefficient(r) where:

$$m = \frac{f_p}{f}$$

$$r = \frac{V_m}{V_{pm}}$$

And in this case we choose : $\begin{cases} m = 0.63 \\ r = 0.8 \end{cases}$

For the first inverter we obtain[25] ,[24] :

$$\begin{aligned} si\ V_{as1ref} \geq V_p(k)\ \ F_1 = 1\ \ sinon\ \ F_1 = 0 \\ si\ V_{bs1ref} \geq V_p(k)\ \ F_2 = 1\ \ sinon\ \ F_2 = 0 \\ si\ V_{cs1ref} \geq V_p(k)\ \ F_3 = 1\ \ sinon\ \ F_3 = 0 \end{aligned} \quad \text{(I.77)}$$

For the second inverter we obtain [25] ,[24] :

$$\begin{aligned} si\ V_{as2ref} \geq V_p(k)\ \ F_4 = 1\ \ sinon\ \ F_4 = 0 \\ si\ V_{bs2ref} \geq V_p(k)\ \ F_5 = 1\ \ sinon\ \ F_5 = 0 \\ si\ V_{cs2ref} \geq V_p(k)\ \ F_6 = 1\ \ sinon\ \ F_6 = 0 \end{aligned} \quad \text{(I.78)}$$

12.4.DSAM ASSOCIATION BY TWO PWM CONTROLLED VOLTAGE INVERTERS

Figure I.14 shows the association of the DSAM with two three-phase voltage inverters with PWM control, the reference voltages are purely sinusoidal.

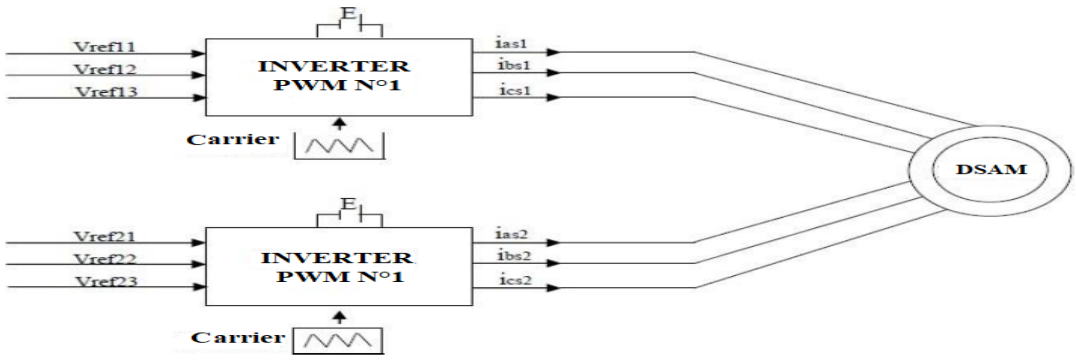

Figure I.14: DSAM Association - PWM Controlled Voltage Inverters [26].

13.SIMULATION RESULTS

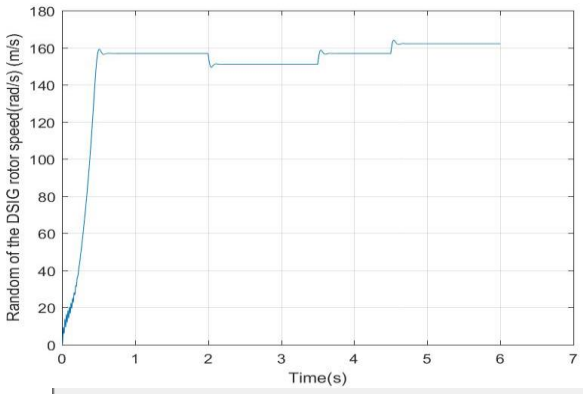

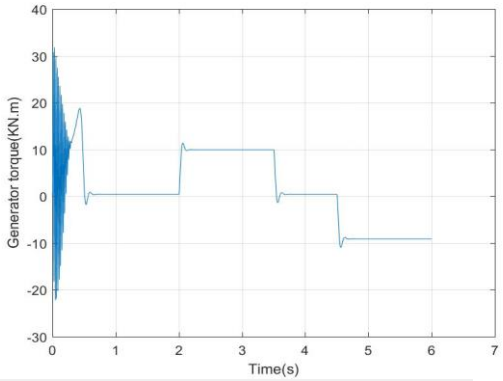

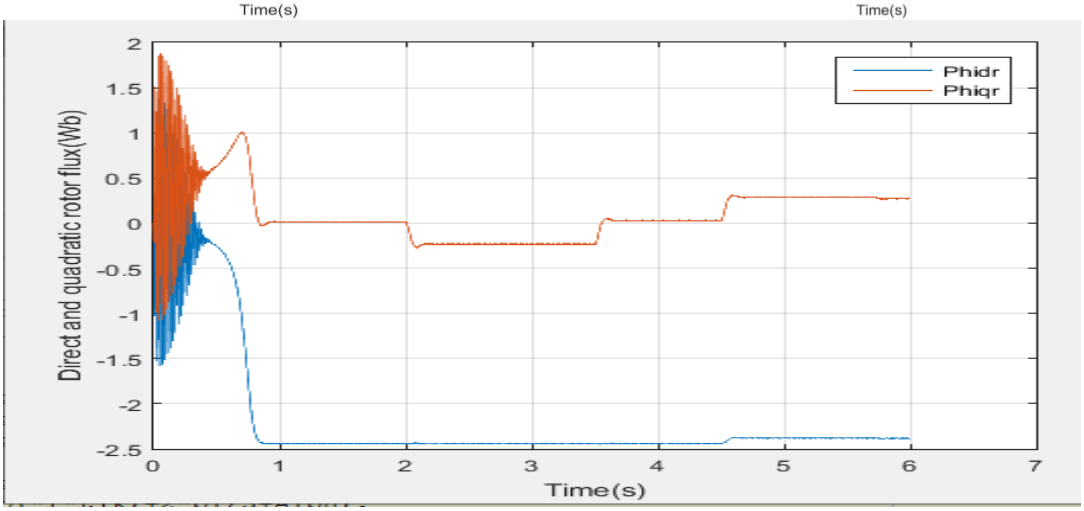

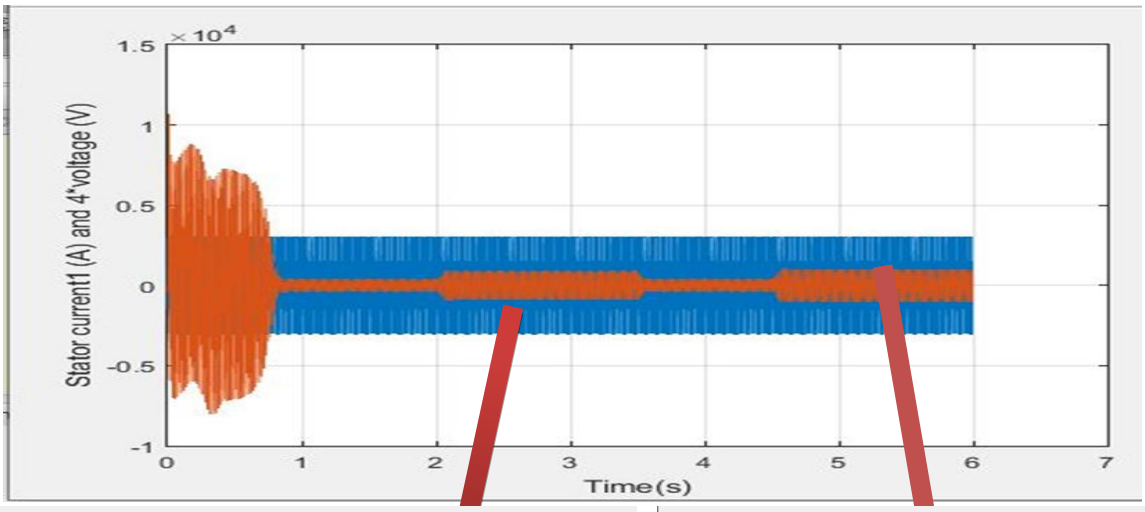

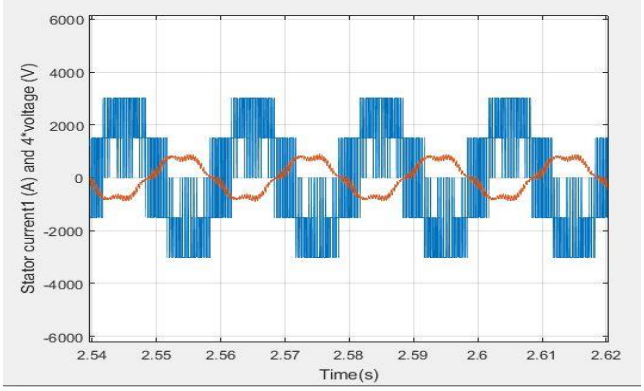

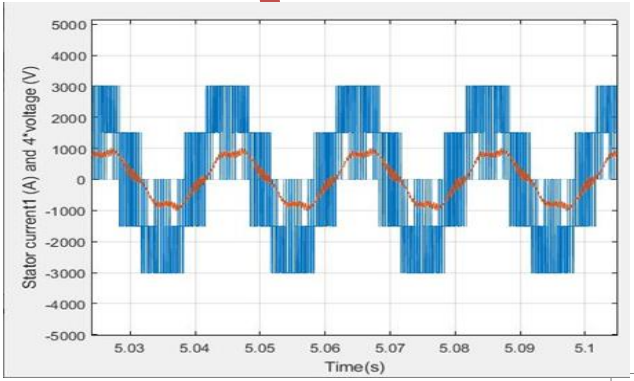

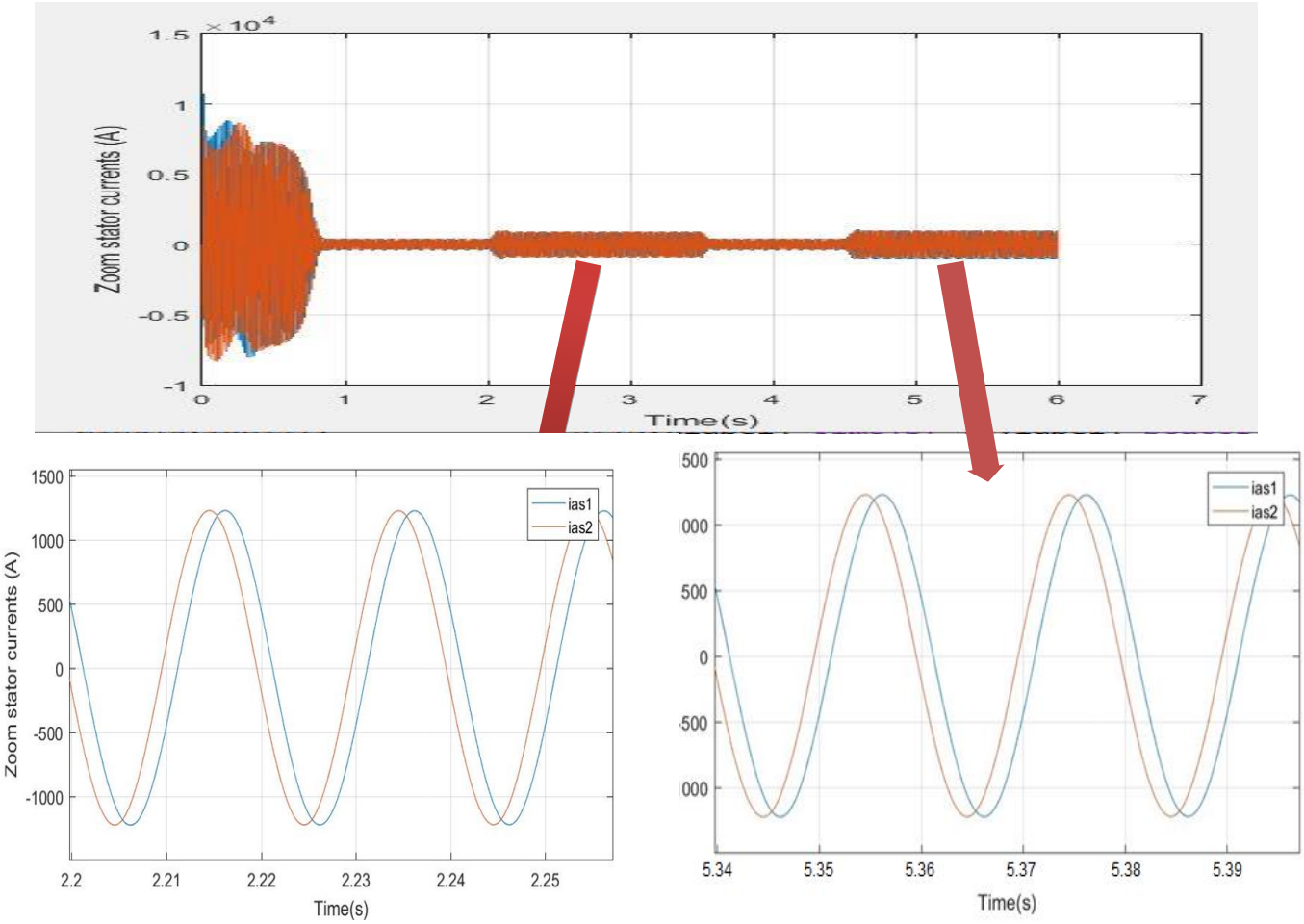

Figure I.15 :Simulation Results.

14.INTERPRETATION

For simulation purposes, the electrical model of a double star induction machine (DSAM) was implemented using Matlab/Command.
Figure I.12 shows the response of the DSAM powered by frequency converters controlled by sinusoidal-triangular PWM (Pulse Width Modulation), with a modulation index **r = 0.8** and **m = 0.63**, followed by the application of nominal loads: $\boldsymbol{C_r}$ = 9550N.m and $\boldsymbol{C_r}$ = −9550N.m Respectively, between time intervals [2, 3.5] and [4.5, 6] seconds, the latter shows that: The DSAM rotational speed increases and evolves in an almost linear manner at the start, then stabilizes and reaches a value of 156.73 rad/s (very close to the synchronous value). We observe the machine's response at t = 2 seconds, showing a significant decrease when a positive resistive torque is introduced, followed by a slight increase at t = 4.5 seconds when a negative resistive torque is introduced. Electromagnetic torque oscillations are observed for 0.5 seconds, corresponding to the initial moments, then decrease in an almost linear manner and stabilize at a value of 390 Nm when it reaches the permanent mode (compensating for frictional losses). At t = 2 seconds and t = 4.5 seconds, the resistive torque values are taken. Stator currents exhibit excessive overshoots at start-up, which are approximately 5 times the rated current, and this is expected. They then decrease and stabilize at steady state, at t = 2 s and t = 4.5 s, and increase slightly under the influence of torque. The evolution of the rotor flux along (d, q) is almost identical to the evolution of the electromagnetic torque. We also note that at t = 2 s, the supply voltage va21 (V) and the stator current ia21 (A) have the same sign, and thus the machine absorbs active and reactive power (necessary for moving and magnetizing the load) from the source (the electrical network). On the other hand, at t = 4.5 s, the stator voltage va21 (V) and the stator current ia21 (A) have opposite signs, and thus the machine supplies active power to the source and absorbs reactive power required for magnetization. We also note that the electrical phase shift angle between the two stars is (α=30°), and this angle is observed through the quantities (voltage and current) along the real axes. The technique used causes increased torque ripples due primarily to the harmonics provided by the reflectors.

15.CONCLUSION

In this chapter, we presented a comprehensive overview of wind energy technology. We began by introducing the main types of wind turbines and the methods used to regulate their output power, including both stall and pitch control techniques. We then explored the main components of wind turbine systems and their power characteristics. A significant focus was placed on the modeling of the dual star asynchronous machine (DSAM), where we derived and analyzed the electrical, magnetic, and mechanical equations governing its behavior. Furthermore, we examined the machine's performance in the two-phase reference frame (Park transformation) and under various reference systems.

In the final sections, we discussed the power supply of the machine and its control using PWM-based voltage inverters. We also detailed how two inverters can be integrated to enhance system performance and concluded with simulation results that validate the proposed models.

However, accurate modeling alone is not sufficient to ensure optimal energy extraction from wind. This is where advanced control strategies come into play, particularly vector control, which is considered one of the most efficient methods for decoupling torque and flux control. It significantly improves the dynamic response and stability of the system. In the next chapter, we will delve into the principles and implementation of vector control, and examine how it can be integrated with the previously established models to achieve maximum power point tracking (MPPT) and overall performance optimization.

CHAPTER 2

VECTOR CONTROL AND SPEED OPTIMIZATION OF DSAM IN WIND ENERGY

CHAPTER 2 : *VECTOR CONTROL AND SPEED OPTIMIZATION OF DSAM IN WIND ENERGY*

1.INTRODUCTION

This technique was first proposed by Blaschke in 1972.The basic idea is to separate the torque and flux componants in the machine,similar to the control of DC motors,which facilitates control and improves accuracy.The method is based on mathematical transformations such as Park-Clark transformations and complex calculations using trigonometric function.

Functions and integrals.Their practical application became possible only with the advent of microprocessors and the development of electronic technology.

The asynchronous machine operates in a manner similar to a separately excited DC machine [29], [30].
This chapter reviews the fundamental concepts and techniques of vector control before applying them to the Dual Stator Asynchronous Machine (DSAM). Subsequently, we examine how to operate the turbine to maximize power generation. Following the presentation and explanation of the simulation results, the performance of this control strategy is analyzed.

2.PRINCIPLE OF THE VECTOR CONTROL

The vector control technique is based on introducing a control law that results in a torque control characteristic similar to that of a separately excited direct current (DC) machine[31] :

$$T_{em} = K.\phi.I_a = K'.I_a.I_f \quad \text{(II.1)}$$

With :

ϕ : Flux imposed by the excitation current I_f

I_a : Armature current .

$K.K'$: Constants.

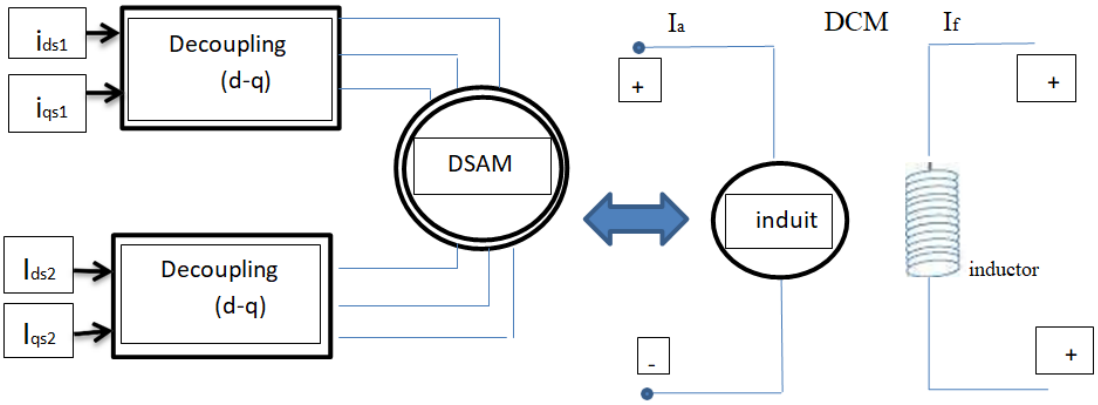

Figure II.1: Principle of vector control for DC motor and DSAM.

The DSAM control process by flux orientation consists of regulating the flux by one component of the current and the torque by the other. To do this, it is necessary to choose a control law and a shaft system that ensures the separation of flux and torque. Note that the electromagnetic torque expression (II.2) is a function of the stator currents and rotor fluxes. However, the electromagnetic torque takes the following form :

$$T_{em} = p\frac{L_m}{L_m+L_r}(i_{qs1} + i_{qs2})\,\phi_{dr} = K''\,\phi_{dr}\,i_{qr}\,. \qquad \text{(II.2)}$$

With :

$$K'' = p\frac{Lm}{Lm+Lr} \quad ; \; i_{qr} = i_{qr1} + i_{qr2}$$

When we reach this equation (II.2), we find that it is similar to the equation of the "DC machine", which explains the separation between torque and magnetic flux in terms of control.

However, while this principle is naturally applied to the DC machine, it is not the case for alternating current machines, particularly the DSAM. In fact, flux-oriented control of these machines requires the orientation of both torque and flux components [32].

3.FLUX ORIENTATION CHOICES

The flux-oriented method is based on the selection of a reference frame, depending on the speed assigned to the (d,q) frame. Consequently, decisions regarding the power supply and the reference frame have been made, including voltage supply and a frame linked to the rotating field. The next step in the reasoning process is to set the flux orientation. To do this, three options are possible [33]:

- Rotor Flux Orientation :

$$\Phi_{dr} = \phi_r \ ; \ \Phi_{qr} = 0 \qquad \text{(II.3)}$$

- Stator Flux Orientation :

$$\Phi_{ds} = \phi_s \ ; \ \Phi_{qs} = 0 \qquad \text{(II.4)}$$

- Orientation of the air-gap flux:

$$\Phi_{dg} = \phi_g \ ; \ \Phi_{qg} = 0 \qquad \text{(II.5)}$$

For the DSAM, we opt for the choice of rotor flux orientation (II.3), because this allows us to obtain a speed variator where the flux and the electromagnetic torque are independently controlled through the stator currents.

4.VECTOR CONTROL METHODS

Can be divided into two main types: direct vector control and indirect vector control :

4.1.DIRECT METHOD

This approach requires precise knowledge of the flow coefficient and its phase,which must be verified regardless of the machine's operating mode [34].To achieve this,the following step are typically employed :

- Measuring the magnetic flux in the machine's air gap using a dedicated sensor.

However ,a major limitation of this technique is the mechanical fragility of flux sensors,making them unsuitable for harsh environments involving strong vibrations or high temperatures.

To overcome this issue,some researchers have turned to estimating the flux using mathematical models.Neverthless,these estimation methods are highly sensitive to variations in the machin's parameters.

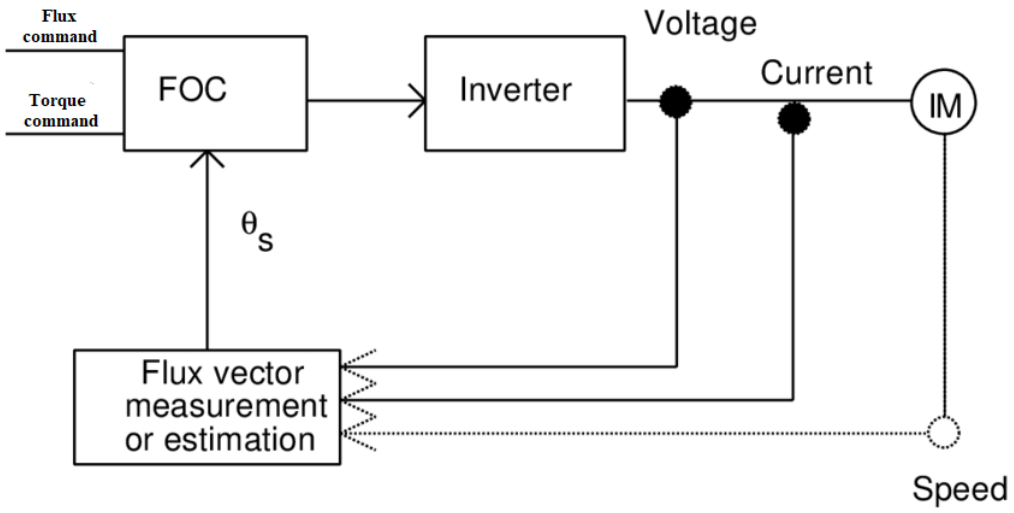

Figure II.2 : Direct vector control method.

4.2.INDIRECT METHOD

The principle of this method is to use only the position of the rotor flux, without relying on its amplitude. The term "indirect method" implies that a flux estimator can be eliminated. However, this method is sensitive to variations in the machine parameters [35].

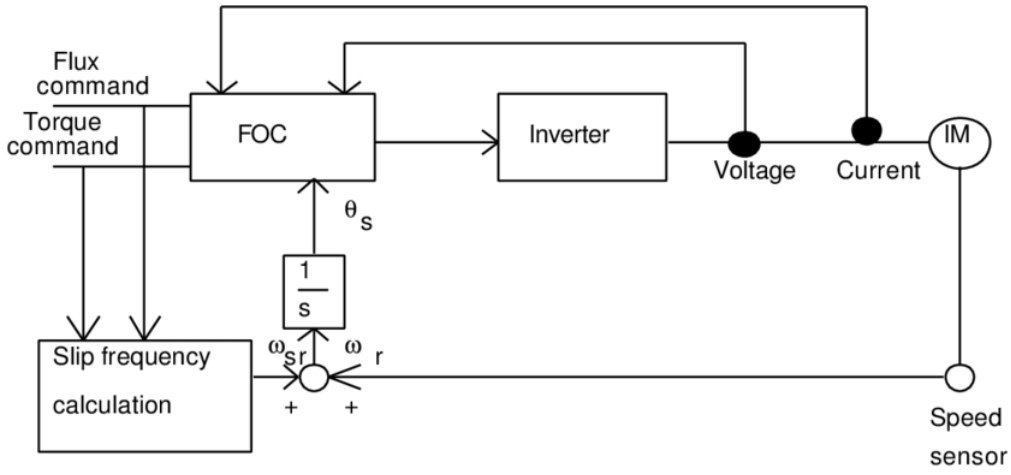

Figure II.3 : Indirect vector control method.

5.SPEED CONTROL OF DSAM

The control laws are derived from the equations governing the operation of the double-star asynchronous machine, and using vector control, we have [04]:

$$\begin{cases} i_{dr} = \frac{\Phi_{dr}}{L_m+L_r} - \frac{L_m}{L_m+L_r}(i_{ds1} + i_{ds2}) \\ i_{qr} = -\frac{L_m}{L_m+L_r}(\Phi_{qr} + (i_{qs1} + i_{qs2}) \end{cases} \quad \text{(II.6)}$$

By applying rotor flux orientation to the system of equations (II.6),we obtain [23]:

$$\begin{cases} i_{dr} = \frac{\Phi_r^*}{L_m+L_r} - \frac{L_m}{L_m+L_r}(i_{ds1} + i_{ds2}) \\ i_{qr} = -\frac{L_m}{L_m+L_r}(i_{qs1} + i_{qs2}) \end{cases} \quad \text{(II.7)}$$

Substituting equation (II.7)into the stator flux equations (I.25),we have:

$$\Phi_{dr} = \lambda_1 \cdot i_{ds1} + L_r\beta i_{ds2} + \beta \cdot \Phi_r^*$$

$$\Phi_{qs1} = \lambda_1 \cdot i_{qs1} + L_r\beta i_{qs2} \quad \text{(II.8)}$$

$$\Phi_{ds2} = \lambda_2 \cdot i_{ds2} + L_r\beta i_{ds1} + \beta\Phi_r^*$$

$$\Phi_{qs2} = \lambda_2 \cdot i_{qs2} + L_r\beta i_{qs1}$$

With :

- $\beta = \frac{L_m}{L_m+L_r}$
- $\lambda_{1,2} = L_{s1,2} + \beta L_r$
- $\Phi_r^* = L_m(i_{ds1} + i_{ds2})$ (II.9)

And : $R_r i_{qr} + \Phi_{sl}{}^* \Phi_r{}^* = 0$ that mean : $i_{qr} = -\frac{\Phi_{sl}{}^* \Phi_r{}^*}{R_r}$ (II.10)

By substituting the second equation (II.8) and equation (II.9) into the system of stator voltage equations, we obtain:

$$V_{ds1}^{*} = R_{s1} i_{ds1} + L_{s1} s i_{ds1} - \omega_s^{*}(L_{s1} \bullet i_{qs1} + \tau_r \bullet \omega_r^{*} \bullet \omega_{sl}^{*})$$

$$V_{qs1}^{*} = R_{s1} i_{qs1} + L_{s1} s i_{qs1} + \omega_s^{*}(L_{s1} * i_{ds1} + \phi_r^{*}) \quad \text{(II.11)}$$

$$V_{ds2}^{*} = R_{s2} i_{ds2} + L_{s2} s i_{ds2} - \omega_s^{*}(L_{s2} * i_{qs2} + \tau_r * \omega_r^{*} * \omega_{sl}^{*})$$

$$V_{qs2}^{*} = R_{s2} i_{qs2} + L_{s2} s i_{qs2} + \omega_s^{*}(L_{s2} * i_{ds2} + \phi_r^{*})$$

With :

$\tau_r = \frac{L_r}{R_r}$ and : $\omega_{sl}^{*} = \omega_s^{*} - \omega_r$

Furthermore we have:

$$\omega_{sl}^{*} = \frac{L_m + L_r}{L_m} * \frac{i_{qs1} + i_{qs2}}{\varphi_r^{*}} \quad \text{(II.12)}$$

$$i_{qs1}^{*} + i_{qs2}^{*} = \frac{L_m + L_r}{L_m} * \frac{T_{em}^{*}}{\phi_r^{*}} \quad \text{(II.13)}$$

The electrical equation system (I.26) indicate that the voltages ($V_{ds1}^{*}, V_{ds2}^{*}, V_{qs1}^{*}, V_{qs2}^{*}$) simultaneously influence both the direct and quadrature components of the stator currents (i_{ds1} , i_{qs1} , i_{ds2} , i_{qs2}) ,there by affecting e both the magnetic flux and the electromagnetic torque. Consequently, decoupling is required. This can be achieved by introducing new variables (V_{ds1r} , V_{qs1r} , V_{ds2r} , V_{qs2r}) which are designed to act independently on the respective stator current components as follows :

$$V_{ds1r} = R_{s1}\, i_{ds1} + L_{s1} s i_{ds2}$$

$$V_{qs1r} = R_{s1}\, i_{qs1} + L_{s1} s i_{qs2} \quad \text{(II.14)}$$

$$V_{ds2r} = R_{s2}\, i_{ds2} + L_{s2} s i_{ds1}$$

$$V_{qs2r} = R_{s2}\, i_{qs2} + L_{s2} s i_{qs1}$$

To compensate for the error introduced during decoupling ,The reference stator voltages under constant flux conditions are expressed as follows,to according to [36]:

$$V^*_{ds1} = V_{ds1r} - V_{ds1c}$$

$$V^*_{qs1} = V_{qs1r} + V_{ds1c} \quad \text{(II.15)}$$

$$V^*_{ds2} = V_{ds2r} - V_{ds2c}$$

$$V^*_{qs2} = V_{qs2r} + V_{qs2c}$$

Given that:

$$V_{ds1c} = \omega^*_s(L_{s1} \bullet i_{qs1} + \tau_r \bullet \phi^*_r \bullet \omega^*_{sl})$$

$$V_{qs1c} = \omega^*_s(L_{s1} \bullet i_{qs1} + \phi^*_r) \quad \text{(II.16)}$$

$$V_{ds2c} = \omega^*_s(L_{s2} \bullet i_{qs2} + \tau_r \bullet \phi^*_r \bullet \omega^*_{sl})$$

$$V_{qs2c} = \omega^*_s(L_{s2} \bullet i_{qs2} + \phi^*_r)$$

Figure II.4 presents a simplified diagram illustrating the speed control mechanism based on vector control :

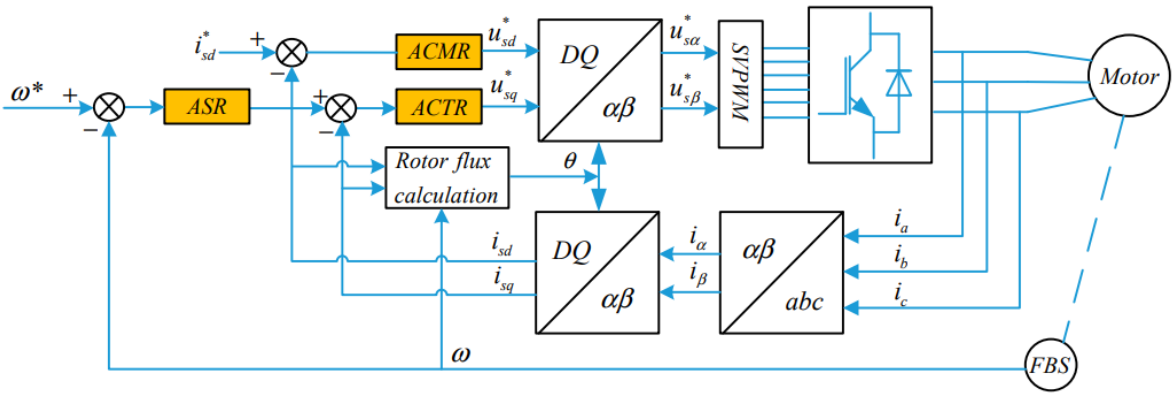

Figure II.4: Vector control structure of an asynchronous motor.

Note :

- ASR: Automatic Speed Regulator.
- ACTR: Automatic Torque Current Regulator.
- ACMR: Automatic Magnetic Field Current regulator .
- SVPWM: Space Vector Pulse Width Modulation.
- FBS : Feedback System.

6.CONTROL OF WIND TURBINE

In wind turbine systems,the control of the convesion of wind kinetic into mechanical energy primarly relies on the dynamic regulation of the turbin's rotational speed.This regulation adapts the generator's behavior to the variations in wind speed,which is considered an external disturbance to the system.In this study,the pitch angle of the blades is assulted to be zero,simplifying the control model while maintaining acceptable effciency[37].

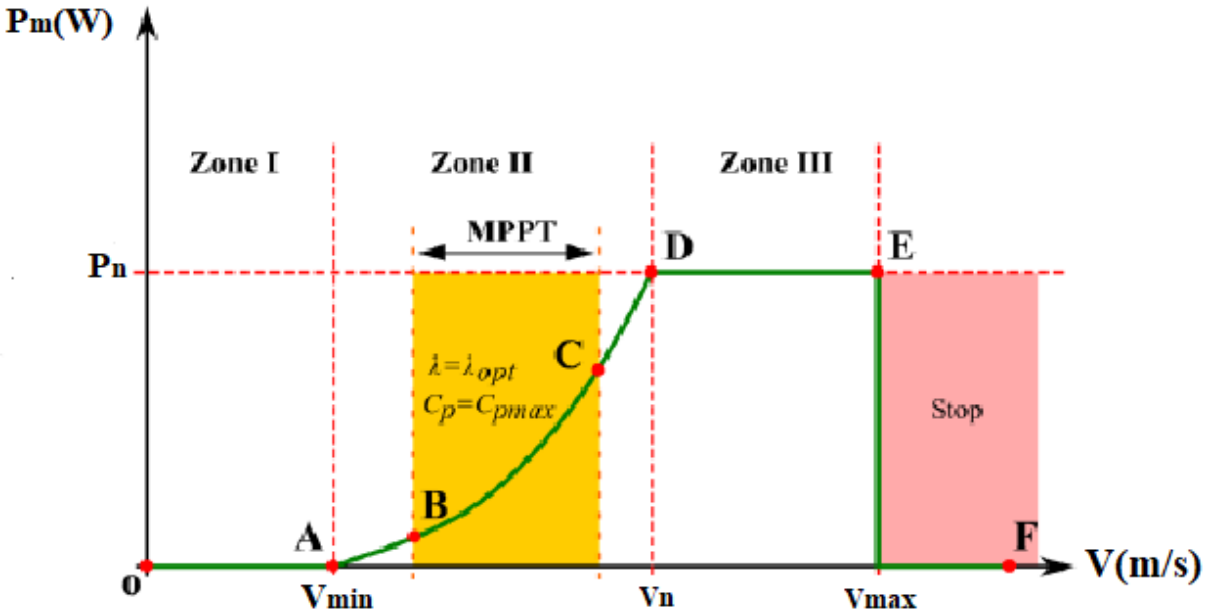

Figure II.5 : Performance appearance of a wind turbine.

The characteristic curve of the power coefficient C_p as a function of the tip speed ratio reveals two key operating zones :

Zone II (ascending) :

This corresponds to the Maximum Power Point Tracking(MPPT)region,where the system aims to adjust the rotational speed to approach the optimal tip speed ratio(OP),maximizing C_p and the energy extracted from the wind[15].

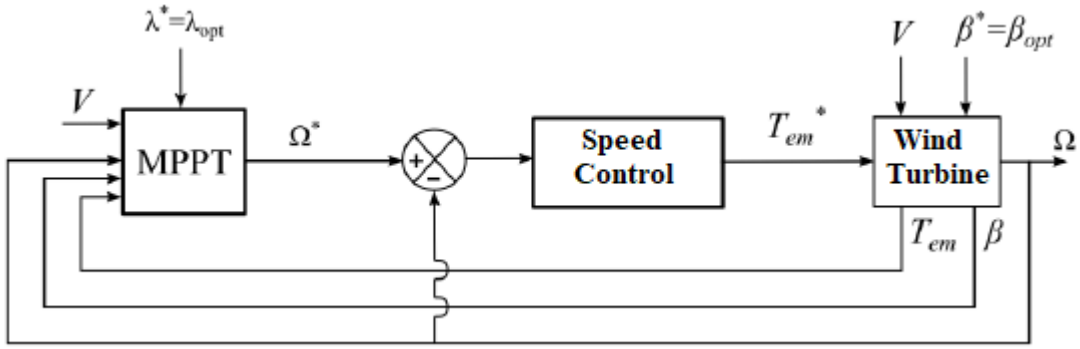

Figure II.6 : Control diagramme for Zone II.

Zone III (descending) :

This represents the operation under constraints,where the speed exceeds the rated value.In this zone,the magnetic flux is intentionally reduced(flux-weakening),lowering the electromagnetic torque and the generated power,thus preventing overloads and protecting the system,particularity the bearings.

The behavior is well illustrated in the functional block diagram of the turbine model,where the control of the electromagnetic torque of the generator ensures the regulation of the rotational speed.In this way,the system adapts in real-time to wind conditions,either to maximize power extraction or to limit the power generared in order to protect the equipment from excessive load[15].

The power extracted from the wind is dependent on the wind speed V,and this relationship can be expressed as follows[01] :

6.1.MAXIMIZATION OF WIND POWER

There exists a specific operating point at which the wind turbine generates maximum power. Achieving and maintaining this optimal point typically requires adapting the electrical load as seen by the generator. This adaptation is often accomplished using a fixed transformer, which must fulfill the following key functions:

- ✓ Minimize power losses as much as possible.
- ✓ Shape the generator's output to match system requirements.
- ✓ Continuously optimize the operating point for maximum power extraction.

This is accomplished by automatically adjusting the load perceived by the generator.Several control strategies can be considered for managing the transformer.A crucial part of this process is determinding the reference torque corresponding to each rotational speed,assuming ideal operating conditions.

The specific speed and torque values are as follows[15]:

$$\Omega_{opt} = \frac{V_{wind}\,\lambda_{opt}}{R}$$

$$T_{em}^{*} = T_{t_{opt}} = K_{opt}\Omega_{opt}^{2}$$

With :

$$K_{opt} = -\frac{1}{2}\frac{C_p^{opt}}{\lambda_{opt}^{3}}\rho\pi R^{5}$$

The control strategy of the system depends on the operating zone.

- **Zone II :**

$$\mathrm{P_{mec}} = \mathrm{P_{mec_{opt}}} = \mathrm{T_{em}^{*}}\Omega_{\mathrm{opt}}$$

- **Zone III :** In order to limit electrical stress on the generator,the reference mechanical power is maintained at its nominal value.Thus,we have :

$$\mathrm{P_{mec}} = \mathrm{P_n}$$

7.FUZZY LOGIC CONTROLLER(FLC)

To achieve efficient vector control of the DSAM, FLCs are used to regulate the currents, speed, and flux due to their simplicity, fast response, and ability to eliminate steady-state error. These controllers also enhance robustness against disturbances. By decoupling the d and q axes, flux and torque can be controlled independently, allowing for quicker system response and improved disturbance rejection. [38],[39],[40].

The FLR issues a command to the process from the error between the setpoint and the regulated output e = $\omega^* - y$.As seen in this figure :

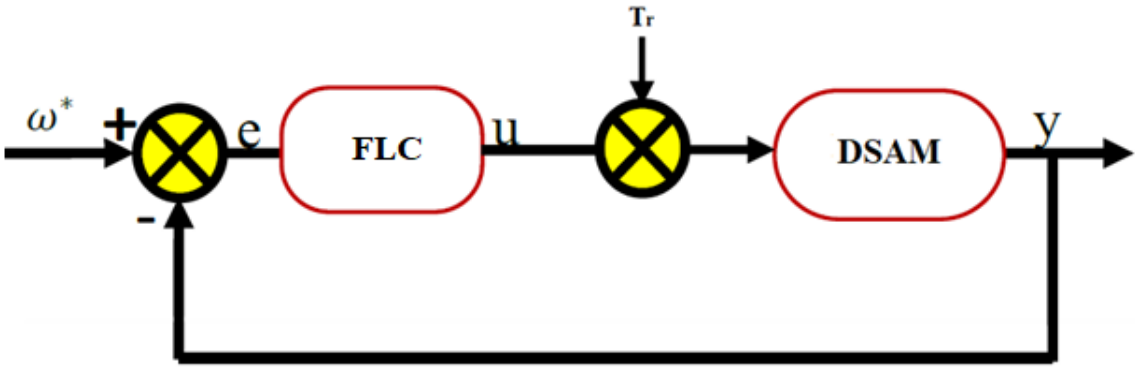

Figure II.7 : General block diagram of a control loop.

The proportional action is defined be the relation:

$$u = K_p(\omega - y)$$

It enhances the speed and accuracy of the response,however,the DSAM experiences greater stress during startup,and the system may become unstable after correction.

7.1.CALCULATION OF PI REGULATOR PARAMETERS

We will explain the procedure on i_{ds1} and the same applies to i_{ds2}, i_{qs1} *and* i_{qs2} .

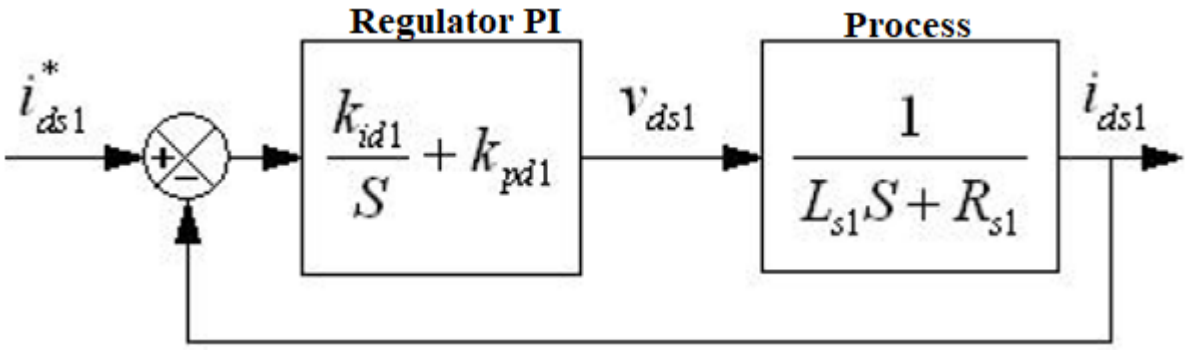

Figure II.8 : Diagram of current regulation.

The transfer function in a closed loop is :

$$\frac{i_{ds1}}{i^*_{ds1}} = \frac{k_{idl} + k_p S}{L_{s1}S^2 + (R_{s1} + K_{pd1})S + k_{id1}}$$

By assigning a pair of complex cunjugate poles $\begin{cases} S_1 = \rho d_1 + j d_1 \\ S_2 = \rho d_1 - j d_1 \end{cases}$

The desired closed-loop characteristic equation can be written as follow :

P(S)= $S^2 + 2_{\rho d1} S + 2\rho_{d1}^2$

So,by definding the PI regulator,we can get the following parameters :

$$K_{pd1} = 2_{\rho d1} L_{s1} - R_{s1}$$

$$K_{id1} = 2\rho_{d1}^2 L_{s1}$$

8.SPEED REGULATOR

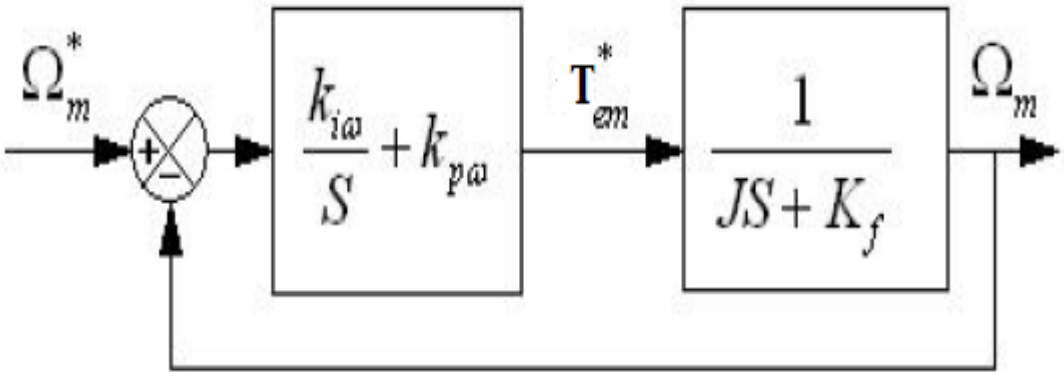

Figure II.9: The simplified regulator speed control.

To estimate the speed controller parameters,we follow the same path we followed to estimate the current controller parameters,in order to obtain:

$$K_{pw} = 2\rho_w J - K_f$$

$$K_{iw} = 2\rho_w^2 J$$

9.SYSTEM OVERVIEW OF VECTOR CONTROL-BASED WIND ENERGY CONVERSION USING DSAM

The figure below illustrates the complete wind energy conversion system employing a Dual Star Asynchronous Machine (DSAM) with vector control and speed optimization strategies.

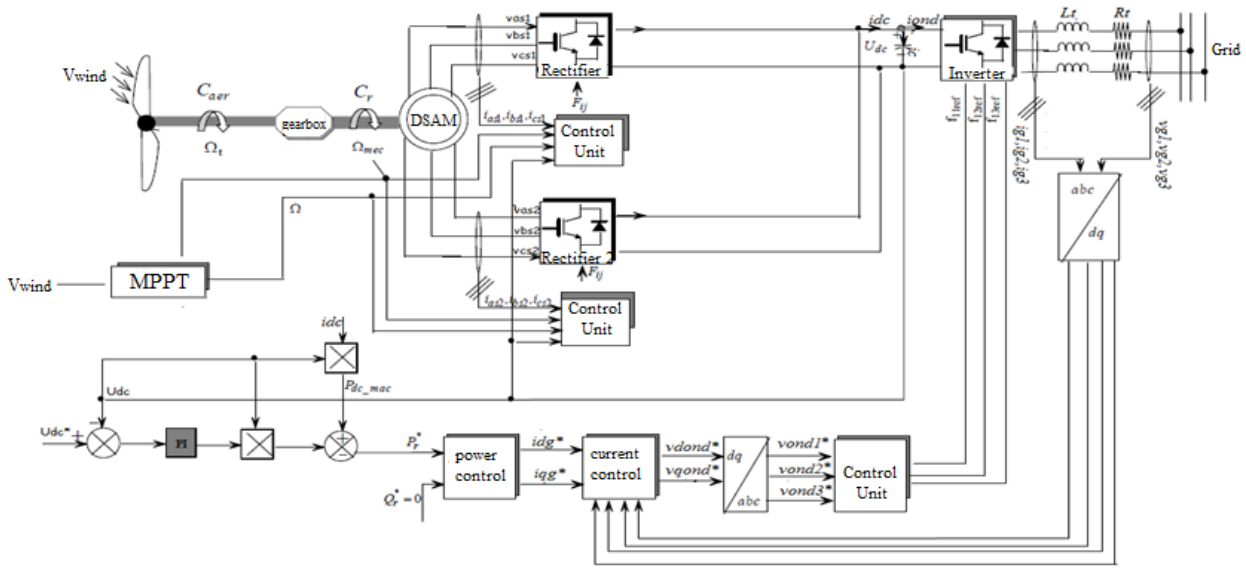

Figure II.10: Diagram of the Studied Wind Energy System and Its Control Strategy.

10.SIMULATION AND INTERPRETATION

Figure (II.11) shows the results obtained from this application, where we were able to extract the following observations:

We note that the machine's electromagnetic torque matches its reference torque, but it differs from the wind speed pattern due to the dynamic torque effect caused by inertia.

The source of the effective power output is clearly demonstrated by the phase shift between the voltage curve and the current curve. This shift is approximately 180 degrees. This is confirmed by the power waves.

The ideal application of the vector control method is demonstrated by the rotor flux curve, which is well-directed, ensuring effective vector control of the machine.

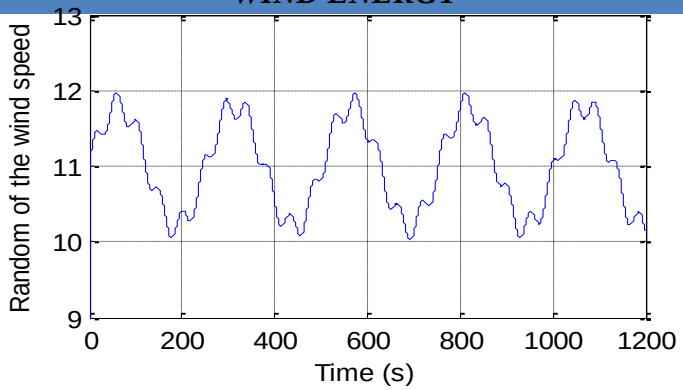
Random of the wind speed
Time (s)

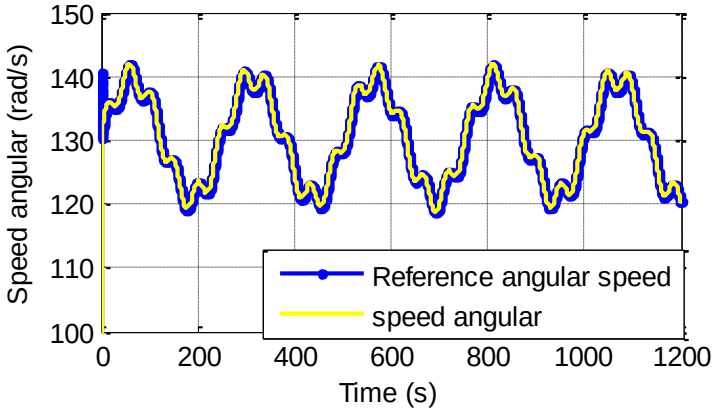
Speed angular (rad/s)
Reference angular speed
speed angular
Time (s)

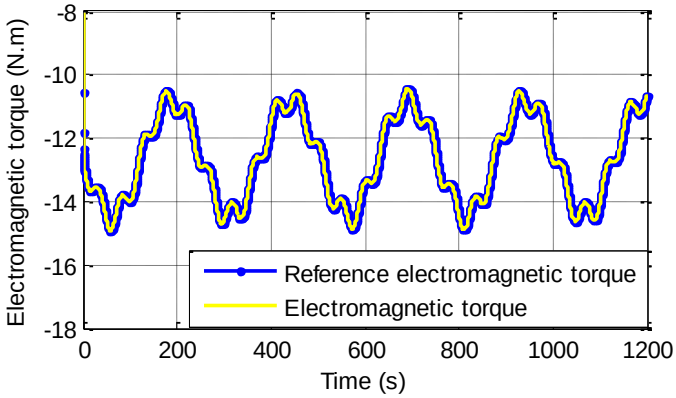
Electromagnetic torque (N.m)
Reference electromagnetic torque
Electromagnetic torque
Time (s)

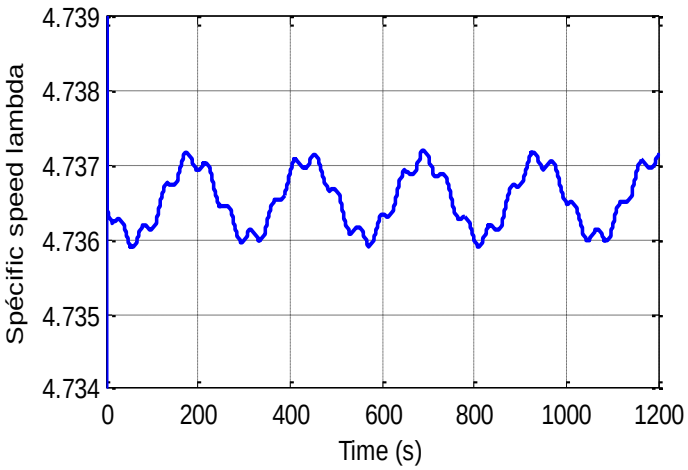
Spécific speed lambda
Time (s)

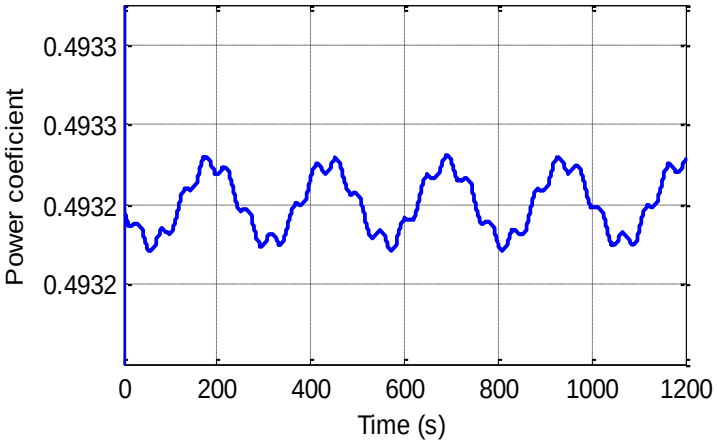
Power coeficient
Time (s)

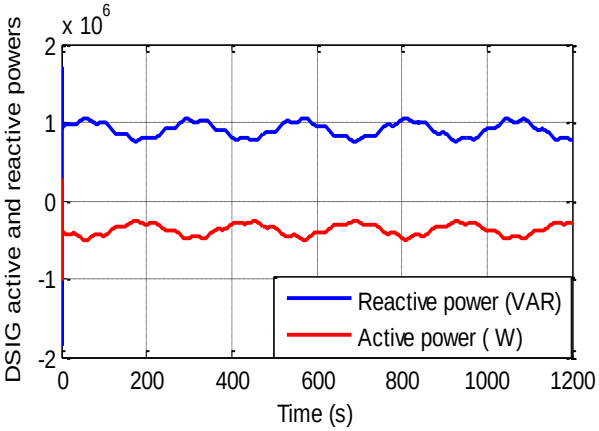
x 10^6
DSIG active and reactive powers
Reactive power (VAR)
Active power (W)
Time (s)

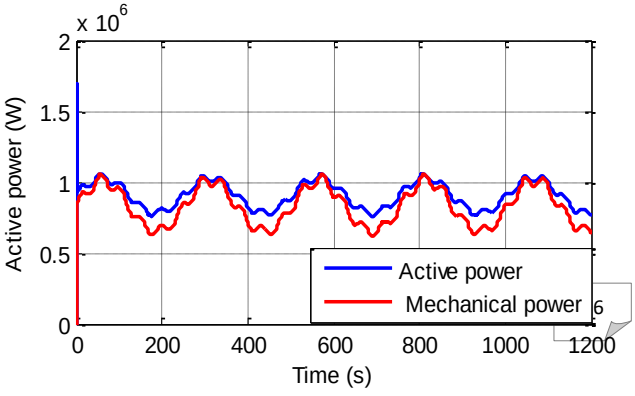
x 10^6
Active power (W)
Active power
Mechanical power
Time (s)

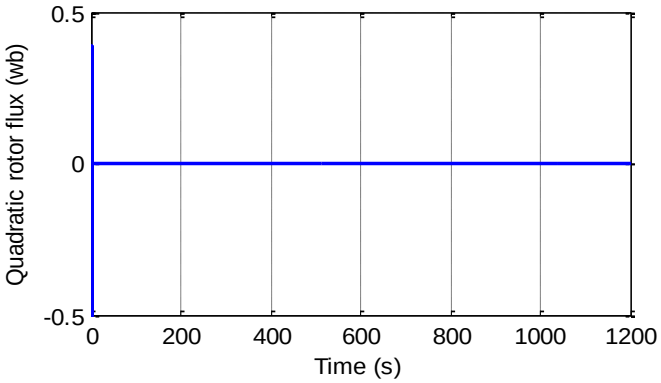

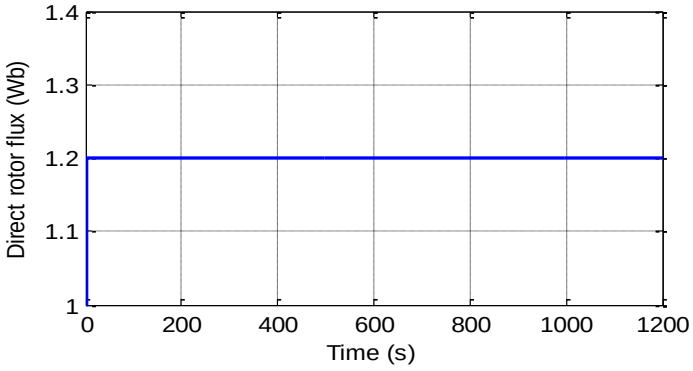

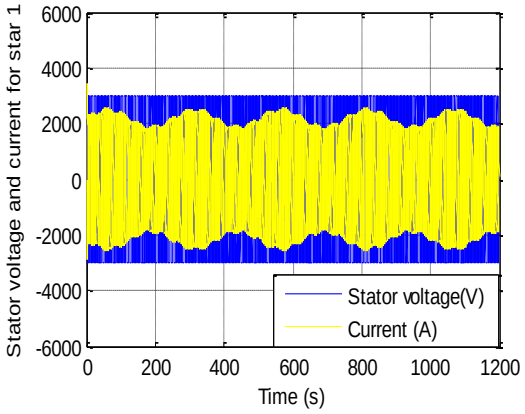

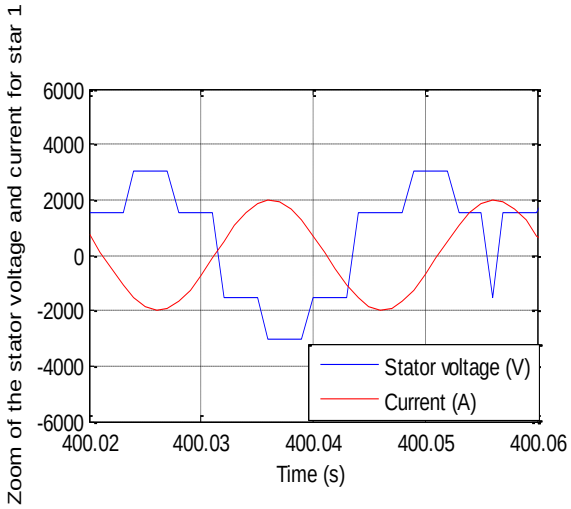

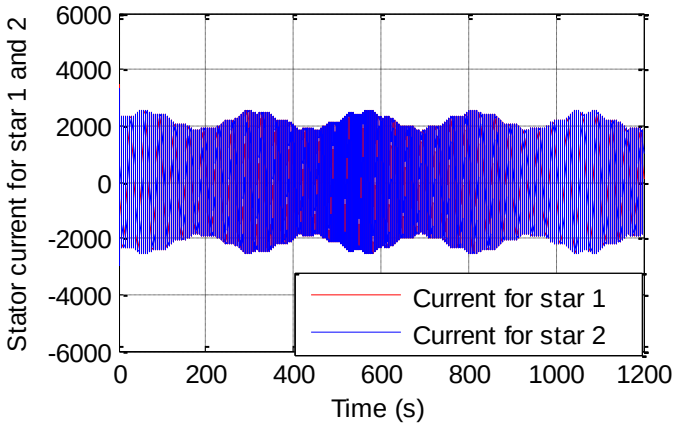

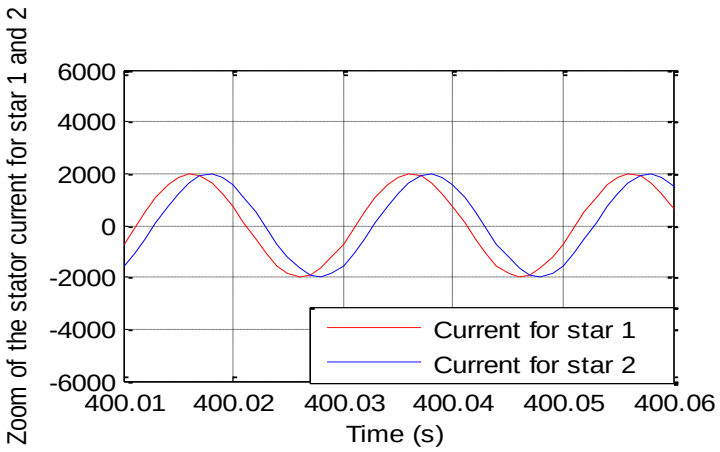

Figure II.11 :Simulation Results.

11.CONCLUSION

In this chapter, the vector control strategy was addressed and applied to the double-star synchronous motor, highlighting the effectiveness of this method in enhancing the performance of the dynamic system. The control was then integrated with the wind turbine to ensure optimal power extraction through speed regulation, following the Maximum Power Point Tracking (MPPT) approach.

The simulation results demonstrated that the proposed control system provides good stability in both speed and torque, and shows an acceptable ability to adapt to variations in wind speed, reflecting the reliability of the adopted regulation strategy. However, some limitations persist, particularly regarding response accuracy and tracking speed in nonlinear conditions or under sudden disturbances.

Therefore, the following chapter will propose the use of fuzzy control as a more flexible alternative approach, aiming to improve system performance and enhance its adaptability to various operating conditions in a more intelligent and robust manner.

CHAPTER 3

FUZZY LOGIC-BASED SPEED CONTROL OPTIMIZATION FOR DUAL STAR ASYNCHRONOUS

1.INTRODUCTION

In everyday life, many situations cannot be described precisely. For example, when we say that a room is "a bit warm" or the speed of a vehicle is "rather slow," we are using vague expressions. Fuzzy logic offers a framework to model this kind of reasoning using so-called linguistic variables and a set of rules that define system behavior [42].

This approach has proven effective in many engineering and industrial applications, especially in the field of automatic control. It has been successfully used in devices such as washing machines, air conditioners, and smart traffic systems [42][43]. In such systems, fuzzy controllers are able to make decisions based on approximate data, similar to how a human would act in uncertain conditions.

One of the strengths of fuzzy logic is that it does not require an exact mathematical model of the system. Instead, it relies on expert knowledge and intuitive rules, which makes it a practical solution for systems that are too complex or too nonlinear for traditional methods [44].

2.HISTORICAL

The first elucidations of Heisenberg's concept of uncertainty, developed by American scientists in the 1920s and 1930s, led to the emergence of fuzzy logic.However, it was in 1965 that Professor Lotfi Zadeh presented the theoretical foundations of this logic in his article entitled "Fuzzy Sets." This internationally renowned automation engineer has since made numerous theoretical advances that have aided in the representation of phenomena in fuzzy terms, overcoming the constraints imposed by the uncertainties of traditional models based on differential equations.

Here is the essence of the history of fuzzy logic [45], [46]:

- In 1973, Lotfi Zadeh proposed the use of fuzzy logic to solve control problems [47].
- In 1975, Professor Mamdani presented the first highly promising application of fuzzy logic control in London and developed a strategy to control a steam boiler [47].
- In 1978, the Danish company F.L. Smidth-Fuller implemented fuzzy logic to control a cement kiln: this was the first real industrial application of fuzzy logic [45], [47].

- In 1983, a water purifier using fuzzy logic was successfully developed.
- Fuzzy logic was introduced by researcher M. Suegno in Japan in 1985. This type of control then became the subject of the first notable achievements developed in the late 1980s and early 1990s, such as the Sendai metro (1987) and the Matsushita Aïsaïgo Pay Fuzzy washing machine (1990). Since then, fuzzy logic has experienced significant growth in Japan, as Japanese companies quickly recognized its benefits from both a technical and commercial perspective [47].

3.BASIC PRINCIPLE OF FUZZY LOGIC

A fuzzy set is characterized by its membership function, which is equivalent to the idea of (characteristic function) [49]. Unlike classical logic, the theoretical foundations of fuzzy logic allow the treatment of imprecise variables having values between 0 and 1, unlike Boolean logic which only allows variables taking the values 0 or 1.

According to standard set theory, an element is either a member of a set or it is not. Therefore, the membership level of an element in a set can only be zero or equal to one. However, according to fuzzy set theory, an element can partially belong to a set. The membership level of an element in a fuzzy set can take any value within the interval [0,1]. The distinction between the two theories lies in the boundaries of the defined sets. According to classical set theory, the boundaries of sets are "sharp," whereas for fuzzy sets, the boundaries are gradual, or even indistinct, as demonstrated in Figure III.1 [49].

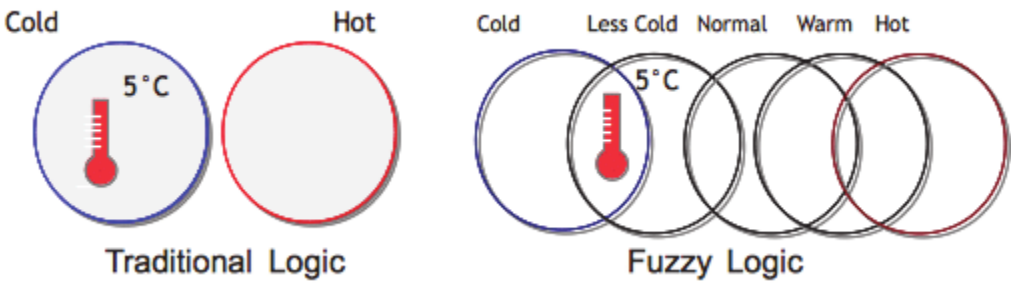

Figure III.1: Comparison between fuzzy logic and classical ensemble.

4.BASIC ELEMENT OF FUZZY LOGIC

4.1.LINGUISTIC VARIABLES

Fuzzy logic handles variables that are imprecise, undefined, or uncertain and emphasizes objective decisions through an approximate reasoning process. These variables constitute linguistic variables, whose values are evaluated or judged using natural language terms or expressions known as fuzzy sets. Linguistic variables, also known as fuzzy variables, represent the input and output parameters to be adjusted in a system. For example, the rotational speed of an electrical machine is a linguistic variable that can simultaneously have multiple values:

(LC) : Less Cold.

(N) :Normal.

(VH) : Very Hot.

4.2.MEMBERSHIP FUNCTION

Is a function that assigns each element of a reference universe a score between 0 and 1, illustrating it's "membership level" in a fuzzy set.

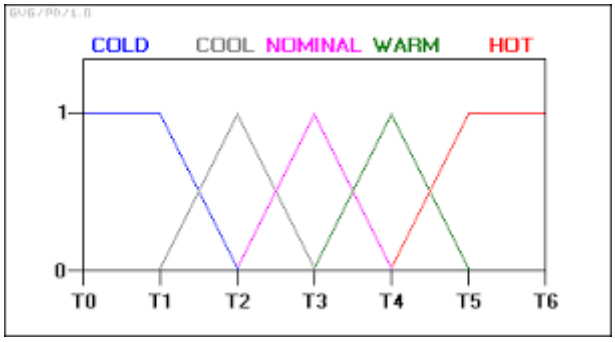

Figure III.2: Fuzzy Membership Functions for Temperature.

Membership Functions for T (temperature) = too-cold, cold, warm, hot, too-hot.

There are different forms of membership functions such as:

- Triangular.
- Trapezoidal.

- Piecewise linear.
- Gaussian.
- Singleton.

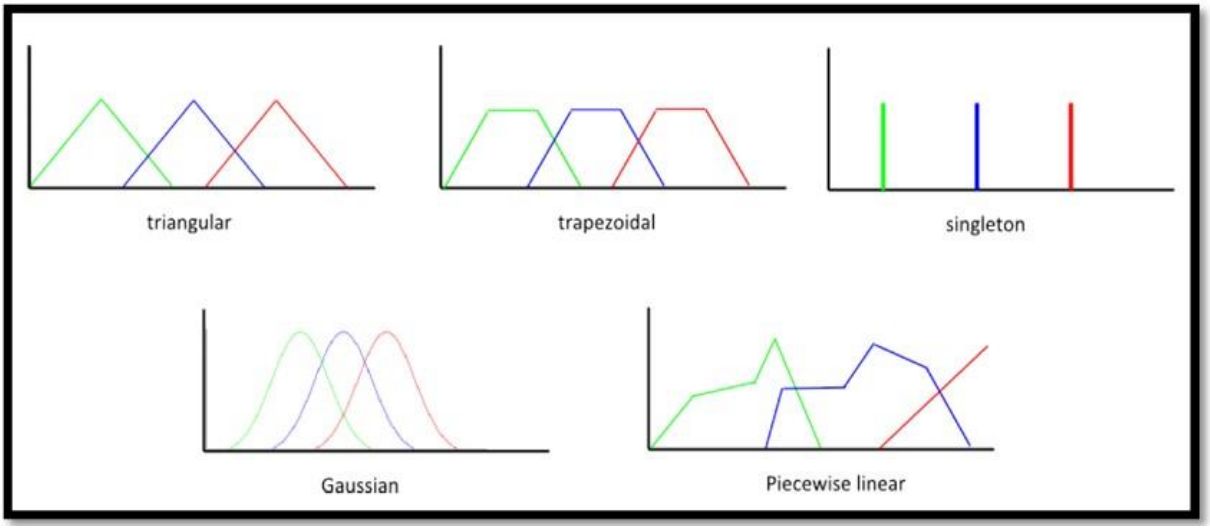

Figure III.3 : Different Types of Membership Functions.

4.2.1.Degree of membership

This value, which is the result of a membership function, is always restricted to the range of 0 and 1. Also referred to as a membership grade or value.

4.3.FUZZY RULES

Expert knowledge makes it possible to infer a proposition or a decision defining a control law—based on one or more fuzzy rules known as inference rules. These rules are connected using fuzzy operators such as:

- AND.
- OR.
- THEN.

They can take the following form:

If condition one AND/OR if condition two THEN decision or action.

In fuzzy rule-based systems that rely on expert knowledge, the logical operator "OR" is generally avoided in the conclusions, as it introduces a degree of uncertainty that may prevent the system from making a clear and reliable decision [50]. Similarly, the use of the "NOT" operator is excluded. For instance, a rule with the conclusion "THEN temperature is NOT high" would be ambiguous, as it does not clarify whether the temperature is low or medium. This lack of precision leads to further uncertainty in the reasoning process.

Therefore, the fuzzy inference mechanism must proceed through four essential stages to reach a final decision.[45]

- the calculation of proposals.
- the calculation of relationships.
- the compositions of the rules with observed facts.
- the aggregation of rules conclusions.

5.FUZZY LOGIC OPERATORS

The mathematical operations for this type of set have been developed with extensive support from those in classical set theory [51],[35]. Basic operations such as intersection, union, integration, and inference are represented by the logical connectives "and," "or," "not," and "then"[51],[15].The following table shows some of the functions commonly used to implement these basic operations. Furthermore, fuzzy inference is constructed from initial fuzzy propositions, and there are many ways to formalize it, the most common of which are also presented in tables [52][53].

Table III.1 : Fuzzy Operators According to Different Theories.

Opérateurs flous	ET	OU	NON
Zadeh (1973)	$Min((\mu_A(x),\mu_B(y))$	$Max\ ((\mu_A(x),\mu_B(y))$	$1-\mu_A(x)$
Lukasiewicz, Giles (1976)	$Max\ ((\mu_A(x),\mu_B(y),-1,0)$	$Min((\mu_A(x),\mu_B(y),1)$	$1-\mu_A(x)$
Hamacher (1978) ; ($\gamma > 0$)	$\frac{\mu_A(x).\mu_B(y)}{y+(1+y)(\mu_A(x)+\mu_B(y),\mu_A(x).\mu_B(y))}$	$\frac{\mu_A(x)+\mu_B(y)-(2-y)\mu_A(x).\mu_B(y))}{1-(1-y)\,\mu_A(x).\mu_B(y)}$	$1-\mu_A(x)$

Table III.2 : Fuzzy implication.

Appellation	Fuzzy implication
Zadeh	Max {min (($\mu_A(x)$, $\mu_B(y)$) ,1-$\mu_A(x)$}
Mamdani	Min ($\mu_A(x)$, $\mu_B(y)$)
Reichenbach	1-($\mu_A(x)$+$\mu_A(y)$.$\mu_B(y)$
Willmott	Max {1-$\mu_A(x)$, min ($\mu_A(x)$, $\mu_B(y)$}
Dièmes	Max (1-$\mu_A(x)$, $\mu_B(y)$)
Brown gold1	Si $\mu_A(x) \leq \mu_B(y)$ $\mu_B(y)$ Otherwise
Lukasiewicz	Min (1,1- $\mu_A(x)$+$\mu_B(y)$)
Larsen	($\mu_A(x)$, $\mu_B(y)$

6.FUZZY LOGIC CONTROL

6.1.STRUCTURE OF A FUZZY CONTROL SYSTEM

In fuzzy logic (RLF) control systems, three main structures can be distinguished:

- The pure structure.
- The Takagi-Sugino-Kang (TSK) structure.
- The Mamdani structure, also known as the "Fuzzing-Defuzzing" model.

In the pure structure, we face two problems: the nature of the input and output variables in the controller is linguistic or fuzzy. However, the input and output variables in real control systems are usually numerical or real variables, which hinders the application of this method.

The TSK structure found a solution to this problem by converting linguistic variables into real variables. However, the outputs are complex and difficult-to-understand mathematical formulas[54].

While the Mamdani architecture proposes adding a defuzzification interface at the end of the pure architecture, the architecture becomes:

- Fuzzification.
- Knowledge base.
- Inference.
- Defuzzification.

The fuzzifier converts the input real variables into linguistic fuzzy variables, while the defuzifier performs the reverse. The Mamdani architecture has become the standard and most widely used model for control applications based on fuzzy logic systems, as illustrated in the following Figure :

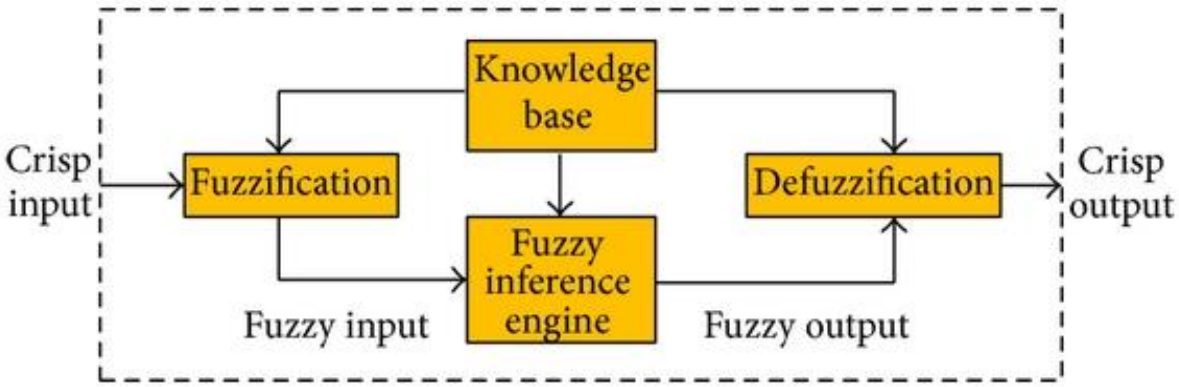

Figure III.4 : Block Diagram of a Fuzzy Controller.

6.2. FUZZIFICATION

Fuzzification is a fundamental step in fuzzy processing, involving the projection of real physical variables onto fuzzy sets representing the corresponding linguistic values [51]. The purpose of this operation is to convert measured or estimated quantities, whether input or output, into linguistic variables expressed by fuzzy terms [26],[55].

To achieve this, the fuzzification block first establishes the value ranges of the membership functions based on the input variable values, then performs the transformation of numerical data into linguistic labels associated with the fuzzy sets. This conversion typically occurs in a normalized domain, such as the interval [−1,1], to simplify calculations [53]. Finally, a matching scale is used to transfer the values to their respective universes of discourse [54].

6.3.KNOWLEDGE BASE

It consists of all the information available to us about the process we want to apply and allows us to define the membership functions and the rules of the fuzzy controller.

6.4.INFERENCE

This operation aims to create a link between the input parameters of the regulator, expressed in linguistic terms, and the output variable in a fuzzy form. This process is based on a thorough understanding and expertise in the operation of the system to be set [56]. Various methods for the numerical processing of inference rules are proposed, including [56], [57],[58].

- Max-min. inference method.
- Max-product inference method.
- Sum-product inference method.

The choice of a particular method depends on the user and the specific case being addressed. In our case, we adopt the product-sum inference method. Assuming that the inputs of the controller are x_1 and x_2, and the output is x_r, the contribution of each rule is given by:

$$\mu_{Ri}(x_r) = \mu(x_1)\mu(x_2)\ \mu_{oi}(x_r) \quad \text{(III.1)}$$

$$= \mu_{ci}\mu_{oi}(x_r) \quad \text{(III.2)}$$

With :

$\mu(x_1)\mu(x_2)$: are the factors of belonging of both linguistic variables x_1 and x_2 in relation to the condition of the rule Ri.

μ_{ci} :is the membership factor of the condition.

$\mu_{oi}(x_r)$: is the membership function of the decision corresponding to the i^{th} rule Ri.

The resulting membership function is given by:

$$\mu_{res}(x_r) = \frac{\mu_{R1}(x_r) + \mu_{R2}(x_r) + \cdots + \mu_{Rm}(x_r)}{m}$$

m: Is the number of rules involved in inference.

6.5.DEFUZZIFICATION

Is the process of transforming a fuzzy output set into a single crisp value. In the context of a Fuzzy Logic Controller (FLC), the defuzzified value represents the control action to be applied to the system. This step serves as the inverse of the initial fuzzification process.

The following are the most commonly used methods for performing defuzzification:

- Center of Sums Method (COS) .
- Center of gravity (COG) / Centroid of Area (COA) Method .
- Center of Area / Bisector of Area Method (BOA) .
- Weighted Average Method .
- Maxima Methods .
    - First of Maxima Method (FOM) .
    - Last of Maxima Method (LOM) .
    - Mean of Maxima Method (MOM).

In this study, we will choose to work on the center of gravity method.Although there is no specific method for choosing between methods, this method is the most widely used.

7.DEFUZZIFICATION BY THE CENTER OF GRAVITY METHOD

The strategy of this method involves graphically processing the areas associated with the membership functions of the linguistic terms in the rule conclusions, denoted as $\mu_{ri}(x)$, which collectively form the resulting membership function $\mu_{res}(x)$.

These areas are weighted by the degree of truth (or firing strength) of each rule. Therefore, it is logical to consider the numerical output value as the abscissa of the center of gravity of the surface formed by the union of these weighted areas, i.e., the function $\mu_{res}(x)$.

The abscissa of the center of gravity of $\mu_{res}(x)$is given by the following expression:

$$x_{Gr} = \frac{\int_{-1}^{1} x_r \mu_{res}(x_r) dx_r}{\int_{-1}^{1} \mu_{res}(x_r) dx_r}$$

Computing the centroid abscissa x_{Gr} generally involves substantial computational effort. However, this process becomes significantly more manageable when the resulting membership function $\mu_{res}(x)$ is derived using the product-sum inference method,thus justifying the selection of this approach.

8.CENTER OF GRAVITY METHOD ASSOCIATED WITH SUM OUTPUT INFERENCE METHOD

According to relations (III.1) and (III.2) and in a condensed form, $\mu_{res}(x_r)$ is given by:

$$\mu_{res}(x_r) = \frac{1}{m}\sum_{i=1}^{m} \mu_{ci}\,\mu_{oi}(x_r) \qquad \text{(III.5)}$$

Substitute expression (III.5) into (III.4) :

$$\int_{-1}^{1} \mu_{res}(x_r)dx_r = \frac{1}{m}\sum_{i=1}^{m} \mu_{ci} \int_{-1}^{1} \mu_{oi}(x_r)dx_r = \frac{1}{m}\sum_{i=1}^{m} \mu_{ci} S_i$$

And :

$$S_i = \int_{-1}^{1} \mu_{oi}(x_r)dx_r$$

Where S_i is the area of the membership function of the fuzzy subset of x_r corresponding to the i^{th} rule.

As for the numerator of (III.4), it can be simplified as follows:

$$\int_{-1}^{1} x_r \mu_{res}(x_r)dx_r = \frac{1}{m}\sum_{i=1}^{m} \mu_{ci} \int_{-1}^{1} x_r \mu_{oi}(x_r)dx_r = \frac{1}{m}\sum_{i=1}^{m} \mu_{ci} x_{Gi} S_i$$

With : $x_{Gi} = \frac{1}{S_i}\int_{-1}^{1} x_r \ \mu_{oi}(x_r)dx_r$

And :

x_{Gi} : Is the abscissa of the center of gravity of the area S_i .

Finally, the center of gravity of $\mu_{res}(x_r)$is obtained from the following simplified and reformulated discrete expression:

$$x_{Gr} = \frac{\sum_{i=1}^{m} \mu_{ci}\, x_{Gi}\, S_i}{\sum_{i=1}^{m} \mu_{ci}\, S_i}$$

Among the advantages and disadvantages of fuzzy logic control, we can cite [59],[53],[60]:

The main advantages are:

- Does not require a precise mathematical model of the process.
- Allows integration of operator expertise through linguistic rules.
- Effectively handles complex systems with strong nonlinearity and difficult modeling.
- Often delivers improved dynamic performance due to its nonlinear nature.
- Can be applied to fast processes using dedicated processors.

On the other hand, the disadvantages are:

- The potential for the emergence of limit cycles due to nonlinear behavior.
- The precision of the adjustments may often be low.
- The consistency of inferences is not guaranteed a priori, with the possibility of contradictory inference rules.
- The lack of clear guidelines for designing the control system (such as selecting measurable variables, determining fuzzification, inference rules, and defuzzification).

9.SPEED CONTROL OF THE DOUBLE-STAR ASYNCHRONOUS MACHINE WITH ROTOR FLUX ORIENTED BY A FUZZY PI CONTROLLER

Generally, the design of a fuzzy controller for electric drive regulation requires the selection of the following parameters:

- Choice of linguistic variables
- Choice of membership functions
- Choice of the inference method
- Choice of the defuzzification strategy

9.1. BASIC STRUCTURE OF A FUZZY CONTROL

For simple single-input systems, the typical inputs to the fuzzy controller are the control error (the difference between the reference value and the process output) and its rate of change, which captures the system's dynamic behavior. The output represents the increment in the control signal to be applied to the system, corresponding to the reference torque T_{em}^{*}. Most existing fuzzy controllers adopt the basic structure proposed by Mamdani, as depicted in the figure below [61].

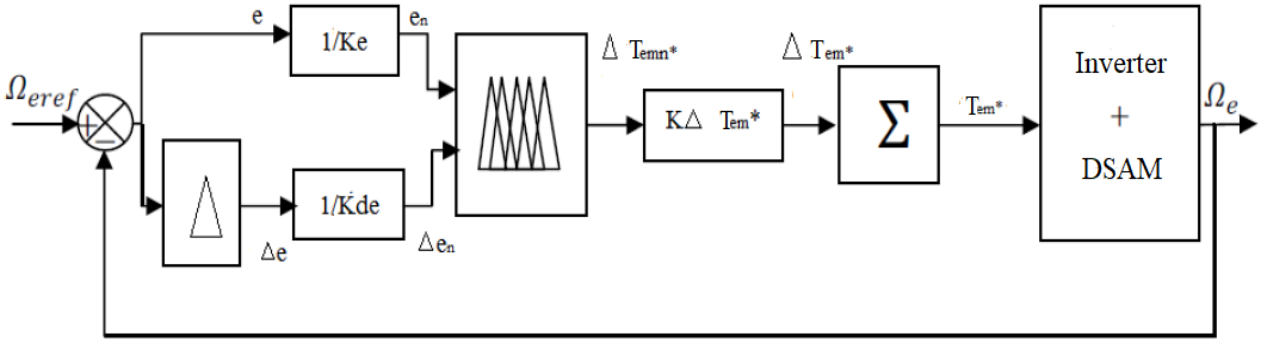

Figure III.5: Block Diagram of a Fuzzy Speed Controller.

The fuzzy controller receives two input variables.

The speed error and its rate of change.

The speed error:

$$e = \Omega_{ref} - \Omega_r$$

The rate of change of the speed error:

$$\Delta e = e_k - e_{k-1}$$

K_e, $K_{\Delta e}$, Δe, and $K_{\Delta Tem}$ are normalization gains, which can be either fixed or adaptive. Selecting them appropriately contributes to maintaining system stability and improving both dynamic response and steady-state performance [62], [63].

Symmetrical triangular membership functions are employed over a normalized universe of discourse within the interval $[-1,1]$ for each variable. This is illustrated in Figures (III.6-a) and (III.6-b), corresponding respectively to the inputs (error and error variation) and the output (reference torque variation):

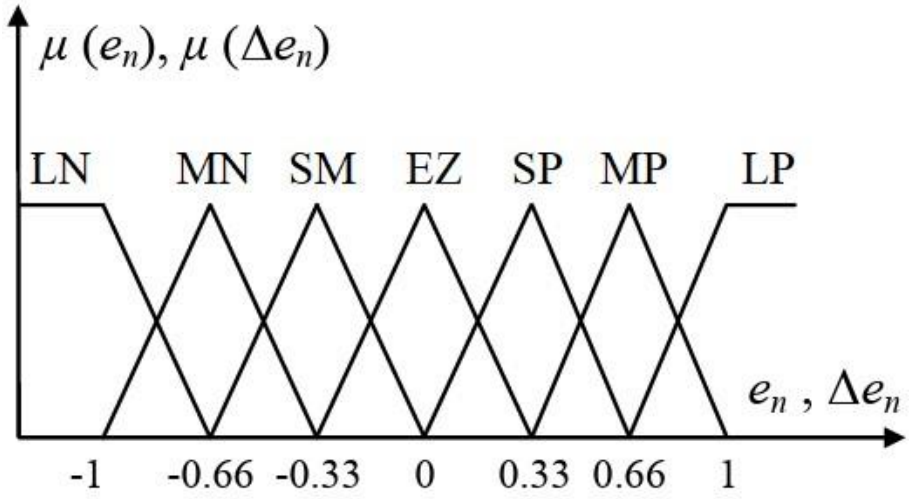

Figures III.6-a : Membership functions of the normalized inputs($e_n, \Delta e_n$).

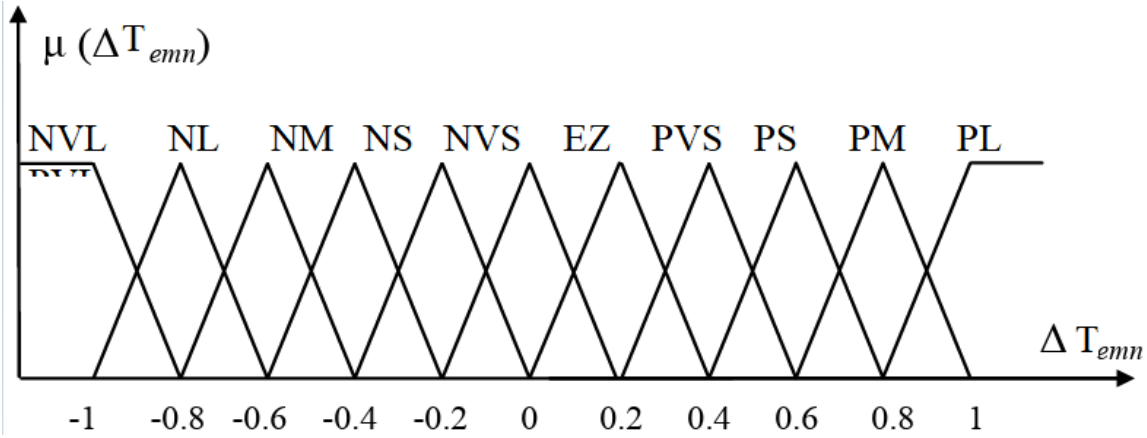

Figures III.6-b : Membership functions of the output variable.

With :

EZ	Equal to Zero	NVS	Negative Very Small
PVS	Positive Very Small	NS	Negative Small
PS	Positive Small	NM	Negative Medium
PM	Positive Medium	NL	Negative Large
PL	Positive Large	NVL	Negative Very Large
PVL	Positive Very Large		

The fuzzy rules, used to determine the output variable of the controller based on the input variables, are derived from the Mac-Vicar inference table. In this case, the table includes a set of 49 rules, as shown in Table III.3.

Table III.3 : Inference matrix.

Δe_n \ e	**NG**	**NM**	**NP**	**EZ**	**PP**	**PM**	**PG**
NG	NTG	NTG	NG	NM	NP	NTP	EZ
NM	NTG	NG	NM	NP	NTP	EZ	PTP
NP	NG	NM	NP	NTP	EZ	PTP	PP
EZ	NM	NP	NTP	EZ	PTP	PP	PM
PP	NP	NTP	EZ	PTP	PP	PM	PG
PM	NTP	EZ	PTP	PP	PM	PG	PTG
PG	EZ	PTP	PP	PM	PG	PTG	PTG

This inference matrix is constructed based on a thorough understanding of the system's behavior and a clear definition of the control objective to be achieved. The defuzzification method used is the center of gravity approach, by which the generated control action is expressed as follows:

$$\Delta T_{emn} = \frac{\sum_{i=1}^{49} \mu_{ci}\, x_{Gi}\, S_i}{\sum_{i=1}^{49} \mu_{ci}\, S_i}$$

Finally, the control action can be expressed as:

$$T_{em}^{*} = T_{em}^{*} + K_{\Delta T_{em}}\, \Delta T_{em}$$

10.SIMULATION

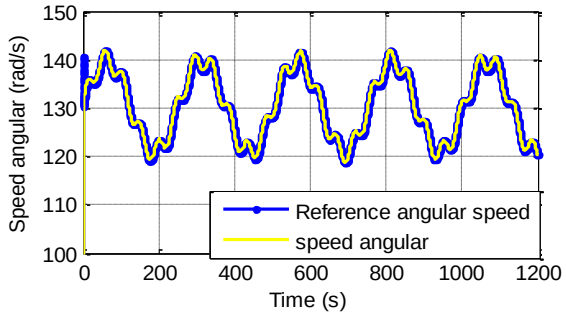

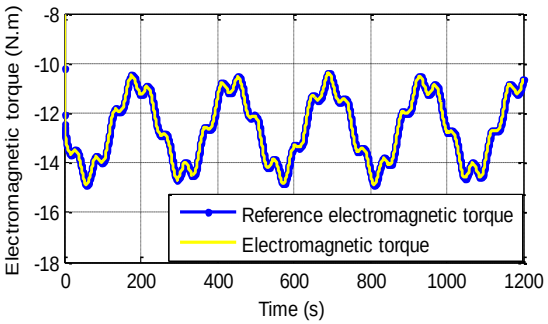

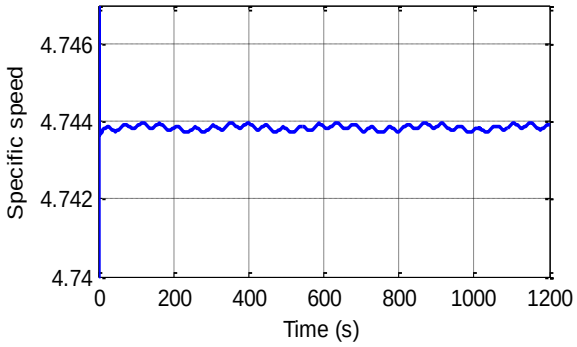

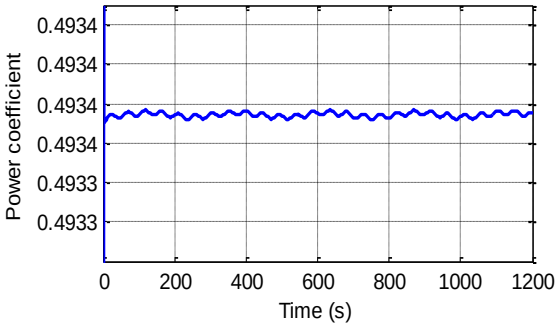

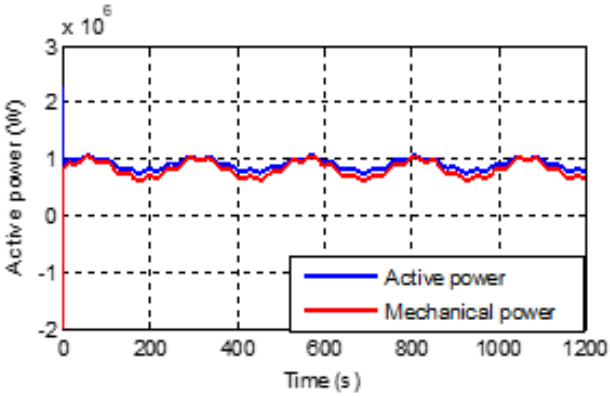

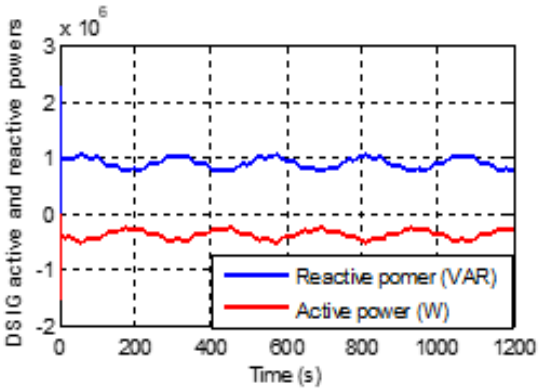

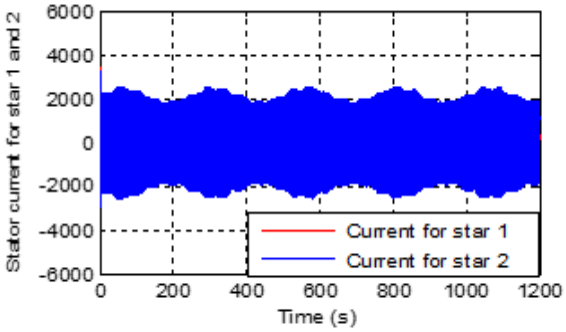

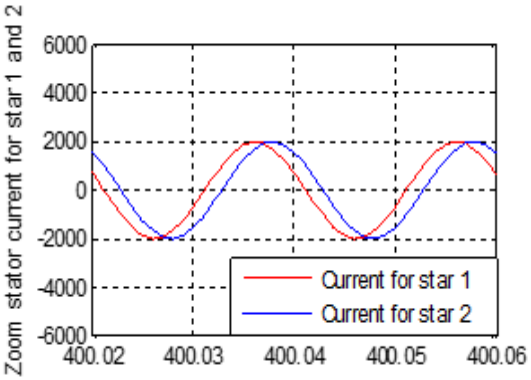

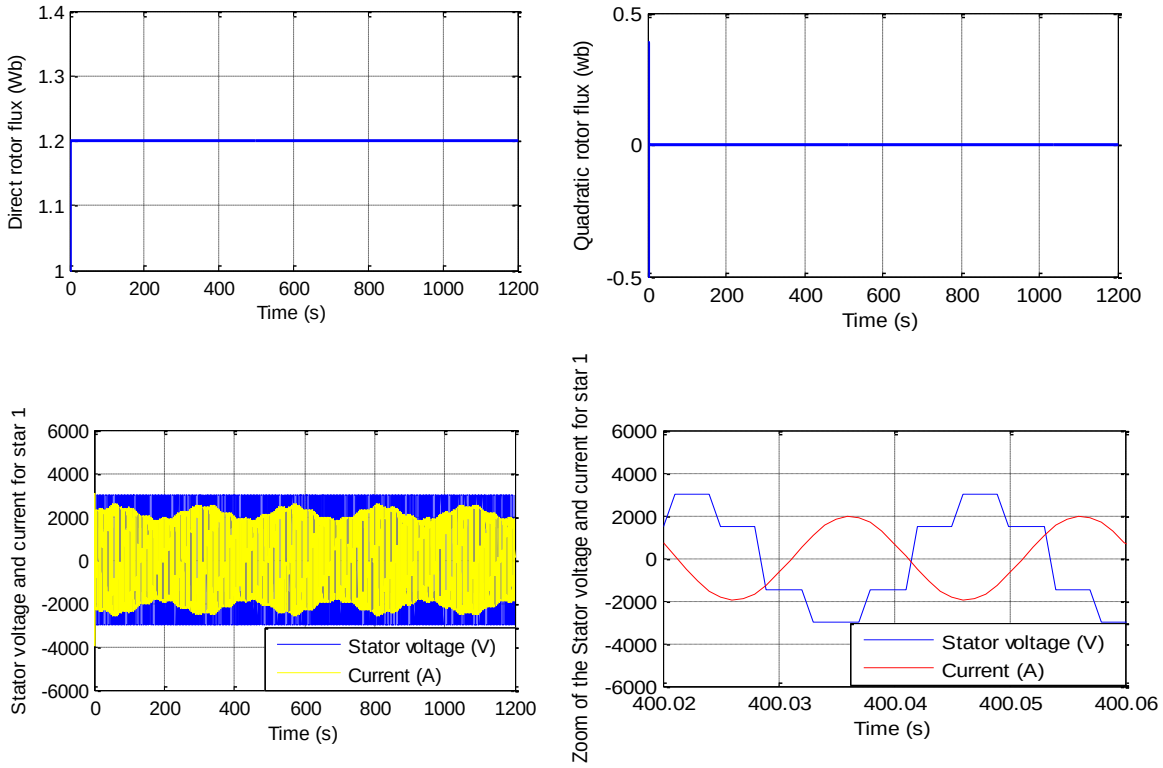

Figure III.7 Simulation Results.

11.INTERPRATATION

The simulation results demonstrate the effectiveness of the fuzzy logic controller in regulating the wind turbine speed and ensuring optimal power extraction through Maximum Power Point Tracking (MPPT). The key observations are as follows:

- The angular speed tracks the reference signal with high accuracy, demonstrating minimal overshoot and fast dynamic response, even under fluctuating operating conditions. This highlights the effectiveness of the fuzzy controller in maintaining rotational speed stability.
- The electromagnetic torque follows its reference trajectory smoothly, with low oscillations, indicating the controller's ability to generate the required torque for optimal turbine performance.
- The tip speed ratio (λ) remains stable around 4.743 and the power coefficient (Cp) around 0.4833, confirming operation near the maximum power point and efficient aerodynamic performance.
- The active power output is closely matched with the mechanical power, maintaining values near 1 MW, which reflects effective energy conversion and minimal system losses.

- Reactive power remains within acceptable limits, while the active power at the grid connection is stable, ensuring reliable and continuous power injection into the grid.
- The direct magnetic flux is held at 1.2 Wb and the quadrature component stays near zero, indicating precise vector control and magnetic field orientation.
- Stator voltages and currents exhibit clean sinusoidal waveforms with consistent phase relationships, confirming the quality of the electrical output and the system's electromagnetic stability.

12.CONCLUSION

Fuzzy control is recognized as an effective technique due to its capability to manage complex systems without requiring a complete mathematical model. This chapter reviewed the fundamental principles of fuzzy logic, its historical background, and various application fields, along with a detailed description of the fuzzy controller structure. Subsequently, a practical application was implemented on a doubly-fed induction motor with oriented flux to regulate the turbine speed.

The simulation results demonstrated a significant improvement in the dynamic response of the system, as well as enhanced robustness of the controller against parametric variations such as rotor resistance, and non-parametric changes like speed setpoint adjustments and load torque variations. These outcomes highlight the effectiveness of fuzzy control as a reliable alternative to conventional control methods for improving the performance of industrial control systems.

GENERAL CONCLUSION

GENERAL CONCLUSION

This work aimed to provide a comprehensive study on the modeling and control of wind turbine systems, with a particular focus on the dual star asynchronous generator operating under variable-speed conditions.

The study began with an overview of wind turbine technologies, outlining the different types and operational modes, and explaining the technical motivations for selecting the dual star induction generator. The structural and functional components of the wind energy system were then analyzed from both mechanical and electromagnetic perspectives.

A complete mathematical model of the generator was developed, including the fundamental equations for voltages, fluxes, torque, and mechanical dynamics. The (d-q) reference frame representation was adopted to simplify control implementation, and the machine behavior was examined in various reference frames—stator, rotor, and rotating field.

In the practical part, emphasis was placed on the control of the generator using Pulse Width Modulation (PWM). The inverter models were integrated with the machine model, and a suitable control strategy was designed to ensure efficient and stable system operation.

Simulation results confirmed the accuracy of the proposed model and the effectiveness of the control strategy, demonstrating the feasibility of employing this type of generator in renewable energy applications.

To conclude, this study opens several promising research directions, including:

- Exploring advanced control strategies such as Direct Torque Control (DTC) or Model Predictive Control (MPC);
- Developing sensorless control algorithms based on speed and wind estimation;
- Investigating the impact of dual star generators on grid stability and power quality;
- Transitioning from simulation to real-time implementation in industrial wind systems.

ANNEX

Technical Parameters

1. Machine Parameters

The following are the technical parameters of the electrical machine used in this study:

Parameter	Value
Rated Speed	**v_n = 1500 rpm**
Rated Frequency	**f_s = 50 Hz**
Stator Phase Resistance (Star 1 and 2)	**$R_{s1} = R_{s2} = 0.008\ \Omega$**
Rotor Phase Resistance	**$R_r = 0.007\ \Omega$**
Stator Phase Leakage Inductance (Stars 1 and 2)	**$L_{s1} = L_{s2} = 1.34 \times 10^{-4}$ H**
Rotor Phase Leakage Inductance	**$L_r = 6.7 \times 10^{-5}$ H**
Cyclic Mutual Inductance (Stators–Rotor)	**L_m = 0.0045 H**
Moment of Inertia	**J = 100 kg·m²**
Friction Coefficient	**Kf = 2.5 N·m·s/rad**
Number of Pole Pairs	**3**

1. Wind Turbine Parameters

The wind turbine parameters considered in this work are presented in the following table:

Parameter	Value
Turbine Radius	R = 36 m
Moment of Inertia	J = 30 kg·m²
Gear Ratio	G = 90
Maximum Power Coefficient	Cp_max = 0.5
Optimal Tip Speed Ratio	λ_opt = 9

BIBLIOGRAPHY

[1] Dekali.Zouheyr , " Contribution à la commande d'un simulateur HIL d'éolienne et d'une génératrice asynchrone à double alimentation", THESE Présentée pour l'obtention du grade de DOCTORAT 3ème Cycle,2021.

[2] R. H. Clark, *Elements of Tidal-Electric Engineering*. Hoboken, NJ, USA: Wiley-IEEE Press, 2007.

[3] Wu, B., Lang, Y., Zargari, N., & Kouro, S. (2011). Power Conversion and Control of Wind Energy Systems. IEEE Press & Wiley.

[4]A.FATIMA ," contribution des techniques de l'intelligence artificielle pour differentes commandes d'une eolienne asynchrone double etoile connectee au reseau electrique ",these de doctorat lmd en systemes electroniques,2017.

[5]T.BELKACEM ," Modélisation et Commande Floue Optimisée d'une Génératrice à Double Alimentation, Application à un Système Eolien à Vitesse Variable ", Présenté en vue de l'obtention du diplôme de Magister,2010.

[6] R. SADOUNI, «Commande par Mode Glissant Flou d'une Machine Asynchrone à

Double Commande par Mode Glissant Flou Machine Asynchrone à Double Etoile».

Mémoire de Magister de l'université D. LIABES de Sidi-bel-abbes, 2010.

[7] H.TAMRABET, "Robustesse d'un contrôle vectoriel de structure minimale d'une

machine asynchrone", mémoire de magister, Université de Batna, 2006.

[8] A. Meroufel, «Commande découplée d'une machine asynchrone sans capteur mécanique», thèse de doctorat, université D.Liabes, Sidi Bel-Abbas, Algérie, 2004.

[9] H.MOHAMMED, " Commande directe du couple d'une machine asynchrone double étoile sans capteur mécanique par les techniques de l'intelligence artificiell"université djillali liabes, 2017.

BIBLIOGRAPHY

[10] E. Merabet, “Commande floue adaptative d’une machine Asynchrone double étoile”, Mémoire de Magister en Electrotechnique , Université de Betna , 2008.

[11] L.Benalia, "Commande en Tension des Moteurs à Inductions Double Alimentés". Thèse de Doctorat de l’université de Batna, 2010.

[12] Z. BENAISSA, S. BENNENI, «Commande vectorielle de la machine asynchrone double étoile». Mémoire de fin d’études de l’Université M. BOUDIAF de M’sila, Algérie, 2008.

[13] A. BALIOUZ , COMMANDE D’UNE MACHINE ASYNCHRONE DOUBLE ÉTOILE PAR RÉGULATEUR GLISSANT", Mémoire de Fin d’Étude En vue d’obtention du diplôme de master,2023.

[14] H . RAHALI , « Commandes non linéaires hybrides et robustes de la machine

asynchrone à double étoile « MASDE » », these de doctorat, Spécialité Génie Electrique,

Université de M’sila 2020, page04.

[15] F.AMEUR," COMMANDE FLOUE OPTIMISEE D’UNE GENERATRICE ASYNCHRONE DOUBLE ETOILE UTILISEE DANS UN SYSTEME EOLIEN A VITESSE VARIABLE", Mémoire de MASTER Domaine,2012.

[16] M.HADJ MAHAMMED Mohammed and M.SAID Abdellah," Modélisation, Alimentation et Commande de la machine asynchrone double stator (MASDS) ", Mémoire présenté en vue de l’obtention du diplôme de MASTER ,2020.

[17]N.HAMDI," Amélioration des performances des aérogénérateurs ", Présenté en vue de l’obtention du diplôme de doctorat en sciences en Electrotechnique,2013.

[18] KERCHA., "Etude et modélisation des machines électriques double étoile " Mémoire Master académique UNIVERSITÉ KASDI MERBAH OUARGLA.2013.

[19] D. Beriber, "Machine asynchrone à double stator alimentée par onduleurs à trois niveaux à structure NPC", Mémoire de Magister, ENP Alger, 2004.

[20] Abdessemed R, Kadjoudj M.Modélisation des machines électriques. Presses de l ’Université de Batna; 1997 pp. 338.

BIBLIOGRAPHY

[21].Kheldoun Aissa, «Amélioration des performances d'un variateur de vitesse par moteur asynchrone contrôlé par la méthode à flux orienté», thèse de doctorat, Université de Boumerdès, 2007.

[22] S.Chekkal, " Evaluation des Performances de l'Aérogénérateur à base de la Machine

Asynchrone Double Etoile Connecté au Réseau Electrique ". Mémoire de magistère Université de Bejaia,2011.

[23] H.Amimeur " Commande d'une Machine Asynchrone Double Etoile par Mode de

Glissement". Mémoire de Magister, Université de Batna 2008.

[24] F.AMEUR , " commande floue optimisee d'une generatrice asynchrone double etoile utilisee dans un système eolien a vitesse variable" , Mémoire de MASTER,2012.

[25] I.Kired et I.Mokhtari, " Commande Vectorielle Directe De La Machine Asynchron Double Etoile ". Mémoire d'ingénieure, Université de Laghouat,2010.

[26] M.OUBACHIR Et M.ZEGGAI ," Commande directe du couple (DTC) pour une machine asynchrone à double étoile " , Présenté pour l'obtention du diplôme de MASTER,2021.

[27] LEONHARD. W, « Control Electrical », Springier Verlag Berlin Heidelberg1985, Printed in Germany.

[28] N.HAMDI," Amélioration des performances des aérogénérateurs ", Présenté en vue de l'obtention du diplôme de doctorat en sciences en Electrotechnique,2013.

[29] K.ABED ,''Techniques de commande avancées appliquées aux machines de types

asynchrone'',Thèse de doctorat , Université Mentouri Constantine ,2010.

[30]M.CHEBRE," Contribution à l'amélioration de la commande parmode glissant d'un MAS sans capteurmécanique" , Pour l'obtention du diplôme de Doctorat en Sciences,2013.

[31] S. Tamazoult, Étude comparative de l'alimentation de la machine asynchrone à double alimentation par un convertisseur statique AC/AC à commutation forcée et naturelle, Mémoire de Magister, Université El-Hadj Lakhdar de Batna, Algérie, juin 2005.

BIBLIOGRAPHY

[32] A. Chaiba, Commande par la logique floue de la machine asynchrone à double alimentation alimentée en tension, Mémoire de Magister, Université El-Hadj Lakhdar de Batna, Algérie, novembre 2004.

[33] M. Hamadache et N. Ouaret, « Commande d'un système de pompage photovoltaïque », mémoire d'ingéniorat, Université de Bejaia, 2007.

[34] A. Boglietti, P. Ferraris, M. Pastorelli, C. Zimaglia, “Induction motors field oriented control based on averaged parameters,” In IEEE, 0-7803-1993-1/94., pp. 81–87, 1994.

[35] E. Merabet et A. Belayali, « Commande par logique floue d'une machine asynchrone à double stator », mémoire d'Ingéniorat Université de M'sila, 2005.

[36] E.Merabet, "Amélioration des performances de régulations d‟une machine asynchrone double étoile par les technique de l'Intelligence Artificielle", Thése de Doctorat ,Batna ,2013.

[37] Y.SAHRAOUI and I. BELMOSTEFA ," COMMONDE VECTORIELLE D’UN AEROGENERATEUR ASYCHRONE DOUBLE ETOILE ", Mémoire de Fin d’Etude En vue d’obtention du diplôme de master,2022.

[38] L. Benalia «Commande en tension des moteurs a induction double alimentes», Thèse de Doctorat, Université de Batna, Algérie, 2010.

[39] K. Loukal, « Commande robuste des machines asynchrones a double alimentation a base des systèmes flous type deux », Thèse de Doctorat, Université de M’sila, Algerie 2017.

[40] H.RAHALI," Commandes non linéaires hybrides et robustes de la machine asynchrone à double étoile « MASDE »", Thèse Présentée pour l'obtention du diplôme de DOCTORAT EN SCIENCES,2020.

[41] L. A. Zadeh, “Fuzzy sets,” *Information and Control*, vol. 8, no. 3, pp. 338–353, 1965.

[42] T. J. Ross, *Fuzzy Logic with Engineering Applications*, 3rd ed. Hoboken, NJ, USA: Wiley, 2010.

[43] G. J. Klir and B. Yuan, *Fuzzy Sets and Fuzzy Logic: Theory and Applications*. Upper Saddle River, NJ, USA: Prentice Hall, 1995.

[44] Jang, J. S. R., Sun, C. T., & Mizutani, E. (1997). Neuro-Fuzzy and Soft Computing. Prentice Hall.

[45] Jensen, P.M. (1979). "Industrial Applications of Fuzzy Logic Control". International Journal of Man-Machine Studies, 11(5), 735–748.

[46] F. Michel, ″Application de la Logique Floue dans la Commande des Machines Synchrones à Aimants Permanents″, Thèse Présentée en vue de l'Obtention de la Maîtrise en Sciences Appliquées, Faculté d'Ingénierie, Université de Moncton, Canada, 2007.

[47] L. A. Zadeh, "The role of fuzzy logic in modeling, identification and control," *Modeling, Identification and Control*, vol. 15, no. 3, pp. 191–203, 1994.

[48] A. Ibaliden, P. Goureau, «fuzzy robust speed control of induction motor», in proceeding. ICEM'96, Pt.III, Vigo, Spain, pp. 168-173, 1996.

[49] Ross, Timothy J. (2010). Fuzzy Logic with Engineering Applications. 3rd Edition, Wiley.

[50] F. Chevrie, F. Guely, ″La Logique Floue″, Cahier Technique Schneider, N°191,Mars 1998.

[51] Y. Elbia ″ Commande Floue Optimisée d'une Machine Asynchrone à Double Alimentation et à Flux Orienté ″, Mémoire de Magister, Batna, 2009.

[52] T .Laamayad « Fuzzy Speed Control of a Dual Star Induction Machine »,10emeConférence sur le génie électrique polytechnique Militaire,2017.

[53] Y.LAGGOUN and H.LIMANE, "Commande d'une machine asynchrone double étoile par logique floue ",Mémoire MASTER ACADEMIQUE,2017.

[54] A.BEGHNI and A.BELKHADEM and A.ZOUDJI, "Commande par logique floue f'une eolienne a base de la generatrice asynchrone a double alimentation(GADA)",MEMOIRE en vue de l'optention de diplôme de MASTER en : Energies Renouvelables,2022.

[55] D. Draincov, H. Hellendoorn, M.R. Frank. "An introduction to fuzzy control", springer,

verlag, 1996.

[56] Bühler, H., "Réglage par Logique Floue", Collection électricité, Presses Polytechniques et Universitaires Romandes, 1994.

[57] Barros, J.-C, "Application de la logique Floue à la Commande Optimale du Moteur Asynchrone" , Thèse de doctorat, Université Marseille III, France, 2003.

[58] K.KOUZI," CONTRIBUTION DES TECHNIQUES DE LA LOGIQUE FLOUE POUR LA COMMANDE D'UNE MACHINE A INDUCTION SANS TRANSDUCTEUR ROTATIF", Thèse de Doctorat en Sciences En Electrotechnique,2008.

[59] J. Camille de Barros, ″Application de la Logique Floue à la Commande Optimale du Moteur Asynchrone″, Thèse de Doctorat en Génie Electrique, Université de Droit, d'Economie et des Sciences d'Aix-Marseille, Aix-Marseille III, France, 2003.

[60] H. Buhler, ″Réglage par Logique Floue″, Presses Polytechniques et Universitaires Romandes, Lausanne, Suisse, 1994.

[61] M. Khami, "Amélioration des performances de régulation d'une machine asynchrone à double alimentation par la technique Neuro-flou", Mémoire de master,

université de ouargla, 2013.

[62] Kouzi, K. ; Mokrani, L. ; Naït-Saïd, M.-S., « Un régulateur flou à gains adaptés par logique floue basé sur le contrôle vectoriel indirect pour l'entraînement d'un moteur asynchrone », Revue Internationale de Génie Électrique, Vol. 3, n° 2, 2003, ISSN 1582-4594, pp. 49-54.

[63] Kouzi, K.; Mokrani, L.; Naït-Saïd, M-S., " A New Design of Fuzzy Logic Controller with Fuzzy Adapted Gains Based on Indirect Vector Control for Induction Motor Drive," IEEE-SSST, Annu. Meeting,WestVirginia , USA, pp. 362-366, March. 2003.

[64] B.Toual " Modélisation et Commande Floue Optimisée d'une Génératrice à Double Alimentation, Application à un Système Eolien à Vitesse Variable", Mémoire de Magister, Université de Batna, 2010.